samples by sequence-independent amplification. *Nucleic Acids Res.* 41:e13. doi: 10.1093/nar/gks794

McElroy, K., Thomas, T., and Luciani, F. (2014). Deep sequencing of evolving pathogen populations: applications, errors, and bioinformatic solutions. *Microb. Inform. Exp.* 4:1. doi: 10.1186/2042-5783-4-1

Metzner, K. J., Giulieri, S. G., Knoepfel, S. A., Rauch, P., Burgisser, P., Yerly, S., et al. (2009). Minority quasispecies of drug-resistant HIV-1 that lead to early therapy failure in treatment-naive and -adherent patients. *Clin. Infect. Dis.* 48, 239–247. doi: 10.1086/595703

Metzner, K. J., Rauch, P., von Wyl, V., Leemann, C., Grube, C., Kuster, H., et al. (2010). Efficient suppression of minority drug-resistant HIV type 1 (HIV-1) variants present at primary HIV-1 infection by ritonavir-boosted protease inhibitor-containing antiretroviral therapy. *J. Infect. Dis.* 201, 1063–1071. doi: 10.1086/651136

Nakamura, K., Oshima, T., Morimoto, T., Ikeda, S., Yoshikawa, H., Shiwa, Y., et al. (2011). Sequence-specific error profile of Illumina sequencers. *Nucleic Acids Res.* 39:e90. doi: 10.1093/nar/gkr344

Neuveut, C., and Jeang, K. T. (1996). Recombinant human immunodeficiency virus type 1 genomes with tat unconstrained by overlapping reading frames reveal residues in Tat important for replication in tissue culture. *J. Virol.* 70, 5572–5581.

Ojosnegros, S., Perales, C., Mas, A., and Domingo, E. (2011). Quasispecies as a matter of fact: viruses and beyond. *Virus Res.* 162, 203–215. doi: 10.1016/j.virusres.2011.09.018

Palmer, S., Kearney, M., Maldarelli, F., Halvas, E. K., Bixby, C. J., Bazmi, H., et al. (2005). Multiple, linked human immunodeficiency virus type 1 drug resistance mutations in treatment-experienced patients are missed by standard genotype analysis. *J. Clin. Microbiol.* 43, 406–413. doi: 10.1128/JCM.43.1.406-413.2005

Paredes, R., Lalama, C. M., Ribaudo, H. J., Schackman, B. R., Shikuma, C., Giguel, F., et al. (2010). Pre-existing minority drug-resistant HIV-1 variants, adherence, and risk of antiretroviral treatment failure. *J. Infect. Dis.* 201, 662–671. doi: 10.1086/650543

Park, S. Y., Goeken, N., Lee, H. J., Bolan, R., Dube, M. P., and Lee, H. Y. (2014). Developing high-throughput HIV incidence assay with pyrosequencing platform. *J. Virol.* 88, 2977–2990. doi: 10.1128/JVI.03128-13

Perelson, A. S., Neumann, A. U., Markowitz, M., Leonard, J. M., and Ho, D. D. (1996). HIV-1 dynamics *in vivo*: virion clearance rate, infected cell life-span, and viral generation time. *Science* 271, 1582–1586. doi: 10.1126/science.271.5255.1582

Pessoa, R., Watanabe, J. T., Calabria, P., Felix, A. C., Loureiro, P., Sabino, E. C., et al. (2014). Deep sequencing of HIV-1 near full-length proviral genomes identifies high rates of BF1 recombinants including two novel circulating recombinant forms (CRF) 70_BF1 and a disseminating 71_BF1 among blood donors in Pernambuco, Brazil. *PLoS ONE* 9:e112674. doi: 10.1371/journal.pone.0112674

Peuchant, O., Thiebaut, R., Capdepont, S., Lavignolle-Aurillac, V., Neau, D., Morlat, P., et al. (2008). Transmission of HIV-1 minority-resistant variants and response to first-line antiretroviral therapy. *AIDS* 22, 1417–1423. doi: 10.1097/QAD.0b013e3283034953

Prosperi, M. C., Yin, L., Nolan, D. J., Lowe, A. D., Goodenow, M. M., and Salemi, M. (2013). Empirical validation of viral quasispecies assembly algorithms: state-of-the-art and challenges. *Sci. Rep.* 3:2837. doi: 10.1038/srep02837

Rabi, S. A., Laird, G. M., Durand, C. M., Laskey, S., Shan, L., Bailey, J. R., et al. (2013). Multi-step inhibition explains HIV-1 protease inhibitor pharmacodynamics and resistance. *J. Clin. Invest.* 123, 3848–3860. doi: 10.1172/JCI67399

Robertson, D. L., Sharp, P. M., McCutchan, F. E., and Hahn, B. H. (1995). Recombination in HIV-1. *Nature* 374, 124–126. doi: 10.1038/374124b0

Schirmer, M., Ijaz, U. Z., D'Amore, R., Hall, N., Sloan, W. T., and Quince, C. (2015). Insight into biases and sequencing errors for amplicon sequencing with the Illumina MiSeq platform. *Nucleic Acids Res.* 43:e37. doi: 10.1093/nar/gku1341

Schirmer, M., Sloan, W. T., and Quince, C. (2014). Benchmarking of viral haplotype reconstruction programmes: an overview of the capacities and limitations of currently available programmes. *Brief. Bioinform.* 15, 431–442. doi: 10.1093/bib/bbs081

Shafer, R. W., and Schapiro, J. M. (2008). HIV-1 drug resistance mutations: an updated framework for the second decade of HAART. *AIDS Rev.* 10, 67–84.

Sharp, P. M. (2002). Origins of human virus diversity. *Cell* 108, 305–312. doi: 10.1016/S0092-8674(02)00639-6

Sharp, P. M., and Hahn, B. H. (2011). Origins of HIV and the AIDS pandemic. *Cold Spring Harb. Perspect. Med.* 1:a006841. doi: 10.1101/cshperspect.a006841

Shiino, T., Hattori, J., Yokomaku, Y., Iwatani, Y., Sugiura, W., and Japanese Drug Resistance HIV-1 Surveillance Network. (2014). Phylodynamic analysis reveals CRF01_AE dissemination between Japan and neighboring Asian countries and the role of intravenous drug use in transmission. *PLoS ONE* 9:e102633. doi: 10.1371/journal.pone.0102633

Shimura, K., Kodama, E., Sakagami, Y., Matsuzaki, Y., Watanabe, W., Yamataka, K., et al. (2008). Broad antiretroviral activity and resistance profile of the novel human immunodeficiency virus integrase inhibitor elvitegravir (JTK-303/GS-9137). *J. Virol.* 82, 764–774. doi: 10.1128/JVI.01534-07

Simen, B. B., Simons, J. F., Hullsiek, K. H., Novak, R. M., Macarthur, R. D., Baxter, J. D., et al. (2009). Low-abundance drug-resistant viral variants in chronically HIV-infected, antiretroviral treatment-naive patients significantly impact treatment outcomes. *J. Infect. Dis.* 199, 693–701. doi: 10.1086/596736

Smit, E. (2014). Antiviral resistance testing. *Curr. Opin. Infect. Dis.* 27, 566–572. doi: 10.1097/QCO.0000000000000108

Stekler, J. D., Ellis, G. M., Carlsson, J., Eilers, B., Holte, S., Maenza, J., et al. (2011). Prevalence and impact of minority variant drug resistance mutations in primary HIV-1 infection. *PLoS ONE* 6:e28952. doi: 10.1371/journal.pone.0028952

Taylor, B. S., Sobieszczyk, M. E., McCutchan, F. E., and Hammer, S. M. (2008). The challenge of HIV-1 subtype diversity. *N. Engl. J. Med.* 358, 1590–1602. doi: 10.1056/NEJMra0706737

Thomson, M. M., Perez-Alvarez, L., and Najera, R. (2002). Molecular epidemiology of HIV-1 genetic forms and its significance for vaccine development and therapy. *Lancet Infect. Dis.* 2, 461–471. doi: 10.1016/S1473-3099(02)00343-2

Varghese, V., Wang, E., Babrzadeh, F., Bachmann, M. H., Shahriar, R., Liu, T., et al. (2010). Nucleic acid template and the risk of a PCR-Induced HIV-1 drug resistance mutation. *PLoS ONE* 5:e10992. doi: 10.1371/journal.pone.0010992

Verbist, B. M., Thys, K., Reumers, J., Wetzels, Y., Van der Borght, K., Talloen, W., et al. (2015). VirVarSeq: a low-frequency virus variant detection pipeline for Illumina sequencing using adaptive base-calling accuracy filtering. *Bioinformatics* 31, 94–101. doi: 10.1093/bioinformatics/btu587

Wainberg, M. A., and Brenner, B. G. (2012). The impact of HIV genetic polymorphisms and subtype differences on the occurrence of resistance to antiretroviral drugs. *Mol. Biol. Int.* 2012:256982. doi: 10.1155/2012/256982

Wensing, A. M., Calvez, V., Gunthard, H. F., Johnson, V. A., Paredes, R., Pillay, D., et al. (2014). 2014 update of the drug resistance mutations in HIV-1. *Top. Antivir. Med.* 22, 642–650.

Willerth, S. M., Pedro, H. A., Pachter, L., Humeau, L. M., Arkin, A. P., and Schaffer, D. V. (2010). Development of a low bias method for characterizing viral populations using next generation sequencing technology. *PLoS ONE* 5:e13564. doi: 10.1371/journal.pone.0013564

Yang, X., Charlebois, P., Gnerre, S., Coole, M. G., Lennon, N. J., Levin, J. Z., et al. (2012). *De novo* assembly of highly diverse viral populations. *BMC Genomics* 13:475. doi: 10.1186/1471-2164-13-475

**Conflict of Interest Statement:** The authors declare that the research was conducted in the absence of any commercial or financial relationships that could be construed as a potential conflict of interest.

frontiers in Microbiology

ORIGINAL RESEARCH
published: 03 February 2016
doi: 10.3389/fmicb.2016.00061

# Unique Flap Conformation in an HIV-1 Protease with High-Level Darunavir Resistance

*Masaaki Nakashima[1,2‡], Hirotaka Ode[1‡], Koji Suzuki[1,2], Masayuki Fujino[3], Masami Maejima[1], Yuki Kimura[1,2], Takashi Masaoka[1], Junko Hattori[1], Masakazu Matsuda[1], Atsuko Hachiya[1], Yoshiyuki Yokomaku[1], Atsuo Suzuki[2], Nobuhisa Watanabe[2,4], Wataru Sugiura[1†] and Yasumasa Iwatani[1,5*]*

[1] Department of Infectious Diseases and Immunology, Clinical Research Center, National Hospital Organization Nagoya Medical Center, Nagoya, Japan, [2] Department of Biotechnology, Nagoya University Graduate School of Engineering, Nagoya, Japan, [3] AIDS Research Center, National Institute of Infectious Diseases, Tokyo, Japan, [4] Synchrotron Radiation Research Center, Nagoya University, Nagoya, Japan, [5] Department of AIDS Research, Nagoya University Graduate School of Medicine, Nagoya, Japan

OPEN ACCESS

**Edited by:**
*Akio Adachi, University of Tokushima Graduate School of Medicine, Japan*

**Reviewed by:**
*Youichi Suzuki, Osaka Medical College, Japan*
*Yasuko Tsunetsugu Yokota, National Institute of Infectious Diseases, Japan*

***Correspondence:**
*Yasumasa Iwatani*
*iwataniy@nnh.hosp.go.jp*

**†Present Address:**
*Wataru Sugiura, GlaxoSmithKline, Tokyo, Japan*

*‡These authors have contributed equally to this work.*

**Specialty section:**
*This article was submitted to Virology, a section of the journal Frontiers in Microbiology*

**Received:** *14 December 2015*
**Accepted:** *14 January 2016*
**Published:** *03 February 2016*

**Citation:**
*Nakashima M, Ode H, Suzuki K, Fujino M, Maejima M, Kimura Y, Masaoka T, Hattori J, Matsuda M, Hachiya A, Yokomaku Y, Suzuki A, Watanabe N, Sugiura W and Iwatani Y (2016) Unique Flap Conformation in an HIV-1 Protease with High-Level Darunavir Resistance. Front. Microbiol. 7:61. doi: 10.3389/fmicb.2016.00061*

Darunavir (DRV) is one of the most powerful protease inhibitors (PIs) for treating human immunodeficiency virus type-1 (HIV-1) infection and presents a high genetic barrier to the generation of resistant viruses. However, DRV-resistant HIV-1 infrequently emerges from viruses exhibiting resistance to other protease inhibitors. To address this resistance, researchers have gathered genetic information on DRV resistance. In contrast, few structural insights into the mechanism underlying DRV resistance are available. To elucidate this mechanism, we determined the crystal structure of the ligand-free state of a protease with high-level DRV resistance and six DRV resistance-associated mutations (including I47V and I50V), which we generated by *in vitro* selection. This crystal structure showed a unique curling conformation at the flap regions that was not found in the previously reported ligand-free protease structures. Molecular dynamics simulations indicated that the curled flap conformation altered the flap dynamics. These results suggest that the preference for a unique flap conformation influences DRV binding. These results provide new structural insights into elucidating the molecular mechanism of DRV resistance and aid to develop PIs effective against DRV-resistant viruses.

**Keywords: Darunavir, HIV-1 protease, drug resistance, crystal structure, flap, I50V, protease inhibitor, molecular dynamics simulation**

## INTRODUCTION

At present, more than 20 antiviral drugs are clinically available to treat patients infected with human immunodeficiency virus type 1 (HIV-1). PIs, such as darunavir (DRV; previously known as TMC114), suppress HIV-1 replication by inhibiting the functions of the viral protease (PR). DRV is a second-generation HIV-1 PI and is one of the most potent anti-HIV-1 drugs, owing to its high antiviral activity and high genetic barrier to the generation of resistant viruses (Koh et al., 2003; De Meyer et al., 2005; Surleraux et al., 2005; Ghosh et al., 2006; Dierynck et al., 2007). However, a history of drug-resistant HIV infection and/or experience of treatment-failure with other regimens could raise concerns about the emergence of DRV-resistant virus, which subsequently results in incomplete viral suppression (Koh et al., 2010; Dierynck et al., 2011). The increasing number of these DRV resistance-associated mutations

at baseline raises the risk of developing DRV resistance (Delaugerre et al., 2008). The latest International AIDS Society (IAS)-USA panel list shows 11 mutations associated with DRV resistance: V11I, V32I, L33F, I47V, I50V, I54M/L, T74P, L76V, I84V, and L89V (Wensing et al., 2014). The emergence of DRV-resistant viruses is the most troublesome clinical issue.

The mechanisms underlying DRV resistance must be elucidated to overcome DRV resistance and develop active drugs against DRV-resistant viruses. One valuable approach is to obtain three-dimensional (3D) structure information of PR variants with high-level resistance to DRV. Nonetheless, few reports have published 3D structures of PR variants with high-level resistance to DRV (Saskova et al., 2009; Agniswamy et al., 2012; Zhang et al., 2014), probably because of the rarity of these PRs. In this study, we generated viruses with high-level resistance to DRV by *in vitro* selection and determined a crystal structure of an HIV-1 PR with high-level resistance to DRV. We obtained a variant with high-level resistance to DRV, which carries I47V and I50V in the PR region. These two mutations are known as the major DRV-resistance mutations (Wensing et al., 2014), although it has also been reported that they reduce viral PR activity and viral fitness (Pazhanisamy et al., 1996; Maguire et al., 2002; Prado et al., 2002; Liu et al., 2005). The solved high-resolution crystal structure of the viral PR exhibited a unique curling conformation at the flap regions (residues 43–58) (Hornak et al., 2006b) that was not found in the previously reported PR structures. These results provide new structural insights into elucidating the molecular mechanism of DRV resistance and aid to develop PIs effective against DRV-resistant viruses.

# MATERIALS AND METHODS

## Sample Collection

Twenty samples with viral sequences that implied resistance to multiple drugs were selected from patient samples sent to the Japanese Drug Resistance HIV-1 Surveillance Network for regular drug-resistance testing from January 2005 to December 2007 (**Table 1**; Hattori et al., 2010). This study was conducted according to the principles of the Declaration of Helsinki. The Ethical Committee at the National Institute of Infectious Diseases approved the study. All patients provided written informed consent for the collection of samples and the subsequent analyses.

## *In Vitro* Selection of a DRV-Resistant Virus

We infected each virus derived from the patient serum into the R5-MaRBLE cell line (Chiba-Mizutani et al., 2007) and induced resistance by treating with 2 nM DRV. The cultures were maintained by changing half of the medium every 3–5 days and by step-wise increases in the DRV concentration to 1000 nM.

## *In Vitro* Phenotype Assay to Examine Drug Susceptibility

The susceptibilities to the PIs were evaluated using an in-house drug susceptibility assay with the R5-MaRBLE cell line as

**TABLE 1 | Twenty multi-drug resistant HIV-1 isolates from clinical samples selected in this study.**

| Patient ID | Exposed PIs | Genotypic resistance mutations | | |
|---|---|---|---|---|
| | | Major | Minor | Other* |
| FS492 | SQV, IDV | I54V, V82F, L90M | G16E, K20I, I62V, L63P | 8 |
| FS796 | IDV, NFV | M46I, V82F, L90M | L63P, H69K | 3 |
| FS1041 | RTV, NFV | V32I, I54V, V82M, L90M | K20R, K43T, M36I, I62V, L63P, A71V, G73S | 3 |
| FS1120 | SQV, RTV | I54V, V82S, L90M | L10I, L33F, Q58E, L63P, A71V, G73S | 2 |
| FS1182 | SQV, NFV | L90M | K20KM, L10I, L63P, A71IV, V77I, G73S | 3 |
| FS1673 | SQV, RTV, IDV, NFV | M46I, I84V, L90M | K20KT, I62IV, L63P, A71V, G73S, V77I | 7 |
| FS1745 | SQV, RTV, IDV, NFV | M46I, I84V, L90M | L10I, M36I, I62V, L63P, A71T, G73T | 7 |
| FS1762 | RTV, DV, NFV | M46I, I54V, V82A | L10I, L24I, L33I, M36L, K43T, I62V, L63P, I64IV | 3 |
| FS1777 | NFV | M46MI, L90LM | L10LI, I62V, L63P, A71AV, G73GS, V77I | 4 |
| FS2510 | SQV, RTV, NFV | D30N, M46I, I54V, N88D, L90M | L10I, L23I, K43T, I62V, L63P, A71T, V77I | 5 |
| FS2628 | SQV, RTV, IDV, NFV | M46I, I84V, L90M | L10I, K20I, M36V, I62V, L63P, A71V, G73S | 3 |
| FS2699 | RTV, NFV | I54V, V82A, L90M | L10I, K20I, M36I, A71V, G73S | 6 |
| FS2715 | IDV, NFV | I54V, V82A, L90M | L10I, M36V, I62V, L63P, A71V, G73T | 2 |
| FS2735 | SQV, RTV, IDV, NFV | M46MI, I84IV, L90LM | L10LI, I62IV, L63P, A71V, G73GS, V77VI | 8 |
| FS5929† | SQV, RTV, IDV, NFV, APV, LPV | M46I, I54V, V82F, L90M | L10I, L23I, L33F, F53L, Q58E, I62IV, L63P, A71V, G73S, V77I | 3 |
| FS6174 | SQV, RTV, NFV | D30N, I54V, N88D, L90M | L10V, K20T, M36I, I62V, L63T, I64IV, A71V | 9 |
| FS6175 | SQV, RTV, LPV, ATV | V32I, M46L, I54V, V82A, L90M | L10V, K20R, M36I, K43KT, F53FL, I62IV, L63P, A71V | 4 |
| FS6189 | NFV | D30N, N88D, L90M | L63P, A71I, V77I | 4 |
| FS6190 | SQV, RTV, NFV, LPV, ATV | M46I, I84V, L90M | L10I, K20T, M36I, F53L, Q58QE, I62V, L63AT, A71V | 8 |
| FS7766 | RTV, APV, ATV | L90M | L10I, L63P, V77I | 3 |

**The column shows the number of PR mutations in each patient other than major and minor mutations.*

*†The multiple drug-resistant virus sample used in this study to induce DRV-resistant HIV-1.*

described elsewhere (Chiba-Mizutani et al., 2007; Shibata et al., 2011). Inhibitory concentration 50% ($IC_{50}$) values were obtained from three independent experiments.

## Extraction and Amplification of Viral RNA

Viral RNA was extracted from the cultured system as follows. First, virus particles in the cell culture supernatant were collected by centrifugation at 20,000 × g at 4°C for 1.5 h. The collected particles were suspended in 300 μL of RNAgents Denaturing Solution (Promega, Madison, WI, USA). Then, the RNA was purified by phenol-chloroform extraction. The *gag-PR* region (625–3402; positions based on HXB2 numbering) of the purified RNA was reverse transcribed using a PrimeScript II High Fidelity One Step RT-PCR Kit (Takara Bio Inc., Kusatsu, Japan). Subsequently, an inner *gag-PR* region (681–3348) was amplified by nested PCR using PrimeSTAR GXL DNA Polymerase (Takara Bio Inc.). The primer sets used for the amplification were as follows: reverse transcription PCR, 5′-ATC TCTAGCAGTGGCGCCCGAACAG and 5′-TACTTCTGT TAGTGCTTTGGTTCC and nested PCR, 5′-CTCTCTCGA CGCAGGACTCG and 5′-TAATCCCTGCATAAATCTGAC TTGC.

## Construction of Recombinant Viruses

A DNA fragment of *gag-PR* region (699–2580) was inserted into the pNL4-3 clone vector using a GeneArt Seamless Cloning and Assembly Kit (Thermo Fisher Scientific, Waltham, MA, USA). First, we amplified the target *gag-PR* region with PrimeSTAR GXL Polymerase. The primer set used for amplification was as follows: 5′-CGGCTTGCTGAAG CGCGCACAGCAAGAGGCGAGGGGCGGCGACTG and 5′-TTACTGGTACAGTCTCAATAGGACTAATGGG. The amplified PCR product was ligated with pNL4-3 without *gag-PR*.

## Construction of the Inactive PR Expression Vector

The full-length *PR* region (2253–2549) was amplified by nested PCR using KOD DNA Polymerase (TOYOBO, Osaka, Japan). The primer set used for amplification was as follows: 5′-ATAT ACATATGCCTCAGATCACTCTTTGG and 5′-TGGTGCTCG AGTTACTAAAAATTTAAAGTGCAGCC. Subsequently, the PCR product was inserted into pET-41a(+) (Merck Millipore, Billerica, MA, USA) using NdeI and XhoI restriction enzymes and a DNA Ligation Kit ver. 2.1 (Takara Bio Inc.). Mutagenesis was performed to obtain an inactive D25N PR mutant.

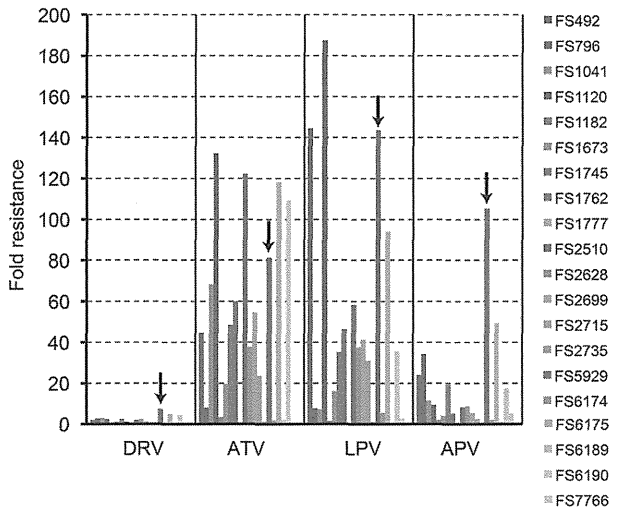


**FIGURE 1 | The PI susceptibilities of 20 clinical HIV-1 isolates.** The arrows in this figure highlight the results for FS5929. The "fold resistance" in $IC_{50}$ are given relative to the $IC_{50}$ values for the reference wild-type HIV-1 JR-CSF, according to the equation, fold resistance = (the $IC_{50}$ against a clinical isolate)/(the $IC_{50}$ against the JR-CSF).

**TABLE 2 | List of PR mutations detected during *in vitro* selection.**

| | | N* | DRV resistance mutations | | | | | | | Other† | | | |
|---|---|---|---|---|---|---|---|---|---|---|---|---|---|
| | | | Major† | | | Minor† | | | | | | | |
| | | | 47 | 50 | 76 | 11 | 32 | 33 | 89 | 54 | 60 | 62 | 82 |
| NL4-3 | | | I | I | L | V | V | L | L | I | D | I | V |
| FS5929 | (Day 0)‡ | | – | – | – | – | – | F | – | V | – | V | F |
| FS5929R | (Day 154)‡ | 4$ | V | V | – | I | I | F | V | V | E | – | F |
| | | 3 | V | V | – | – | I | F | V | V | E | – | F |
| | | 2 | V | V | – | I | I | F | V | V | E | – | L |
| | | 1 | V | – | V | I | I | F | V | V | E | – | F |
| | | 1 | V | – | V | – | I | F | V | V | E | – | F |
| | | 1 | V | – | – | I | I | F | V | A | E | – | F |
| | | 1 | V | – | – | I | I | F | V | V | E | – | F |

*The number of clones with the combination of mutations.*

†*Classification of the IAS-USA mutation list at June/July 2014.*

‡*FS5929 and FS5929R denote the input virus for the in vitro selection (day 0) and the virus mixture obtained at the day 154 in this study.*

*The sequence contains mutations: L10I, L23I, L33F, M46I, F53L, I54V, G57R, Q58E, I62V, L63P, H69R, A71V, G73S, V77I, V82F, L90M, and I93L, compared with NL4-3. L33F is reported to be associated with DRV-resistance mutations.*

$*The major virus in the virus mixture obtained at the day 154 (FS5929R) was defined as FS5929R1.*

## Expression, Purification, and Refolding of the Inactive PR

The enzymatically-inactive PR was expressed, purified, and then refolded by using a method similar to that in the previous report by Dr. Schiffer's group (King et al., 2002). Briefly, the inactive PR was expressed in LB medium with 1 mM IPTG at 37°C. The inclusion bodies with the PR were collected by using a French press and subsequently centrifuged at 10,000 × g at 4°C for 5 min. The collected inclusion bodies were washed with 2 M urea, and the PR protein was solubilized in a 50% acetic acid solution. The obtained PR protein was purified by gel filtration with a HiLoad 26/60 Superdex75 (GE Healthcare Bio-Sciences, Pittsburgh, PA, USA) and AKTAPrime (GE Healthcare Bio-Sciences). The PR was refolded in buffer containing sodium acetate (pH 5.5). Finally, the PR was further purified by gel filtration with a HiLoad 26/60 Superdex75 column (GE Healthcare Bio-Sciences).

## Crystallization of the Inactive PR

The purified PR was concentrated to a final concentration of 2.6 mg $mL^{-1}$ with a VIVASPIN MW5000 concentrator (GE Healthcare Bio-Sciences). Then, initial crystallization conditions of PR were screened using following crystallization screening kits: Wizard I (Emerald Biosystems, Bainbridge Island, WA, USA), Wizard II (Emerald Biosystems), and JCSG-*plus* Screen MD-137 (Molecular Dimensions, Suffolk, UK). The final optimized crystallization condition after iterative optimization cycles was at 0.84 M Lithium chloride, 0.84 mM Sodium citrate, 17%(w/v) PEG 6000, 10% Glycerol, and 5% Ethylene glycol. The crystal was obtained by the hanging-drop vapor-diffusion method. The drops were incubated at 20°C.

## X-ray Diffraction and Data Collection

The X-ray diffraction data were collected at the SPring-8 beamline BL38B1 (Sayo, Hyogo, Japan). The data were integrated with the HKL2000 program (Otwinowski and Minor, 1997). The structure of the inactive PR was determined by the molecular replacement method with the MOLREP programs (Vargin and Teplyakov, 1997; Winn et al., 2011) using a wild-type (WT) PR structure (Protein Data Bank (PDB) ID: 1KJ7) (Prabu-Jeyabalan et al., 2002) as the search model. The structure was further refined with the REFMAC5 and COOT programs (Murshudov et al., 1997; Emsley et al., 2010).

## Molecular Dynamics (MD) Simulations

We performed 30 ns MD simulations of the ligand-free states of the PRs under explicit water conditions. The initial structures of the PRs were generated based on a known crystal structure (PDB ID: 1HHP) (Spinelli et al., 1991) and the structure solved in this study. In the initial structures, the PRs were surrounded by approximately 12,000 water molecules, and N25 was changed to the catalytically active D25. We conducted energy minimization for the PR system by first using 10,000 steps of the steepest descent method and then 10,000 steps of the conjugated gradient method. We subsequently heated the energy-minimized system to 310 K (~37°C) by using the NVT ensemble. Then, we performed MD simulations at 310 K and 1 atm by using the NPT ensemble. During the simulations, hydrogen bonds among residues in the fireman's grip, D25/T26/G27/D25′/T26′/G27′, were retained with a harmonic potential of 100 kcal $mol^{-1}$ $Å^{-2}$ and 100 kcal $mol^{-1}$ $degree^{-2}$.

We also predicted the structures of mutant PRs in complex with DRV with 6.0 ns MD simulations by using a method similar to that in our previous reports (Ode et al., 2007a,b). Briefly, the initial structure of each molecule was generated from a crystal structure of PR in complex with DRV (PDB ID: 1T3R) (Surleraux et al., 2005). We performed 6.0 ns MD simulations of these structures and then estimated the binding energies between PR and DRV by the MMPBSA method using 1000 trajectories from the well-equilibrated final 1.0 ns of the simulations. For the structural comparison, the representative structure among 1000 snapshots taken during the last 1.0 ns of the simulations was used. The formation of a hydrogen bond was defined as described in our previous studies (Ode et al., 2007a,b).

The simulations were conducted with the AMBER9 software package (Case et al., 2006). The ff10 force field (Hornak et al., 2006a) and gaff (Wang et al., 2004) were used to calculate the energies and forces in the simulations.

# RESULTS

## *In Vitro* Selection Yielded Variants that Accumulated DRV Resistance-Associated Mutations

To obtain a crystal structure of an HIV-1 PR with high-level resistance to DRV, we generated a virus with high-level resistance

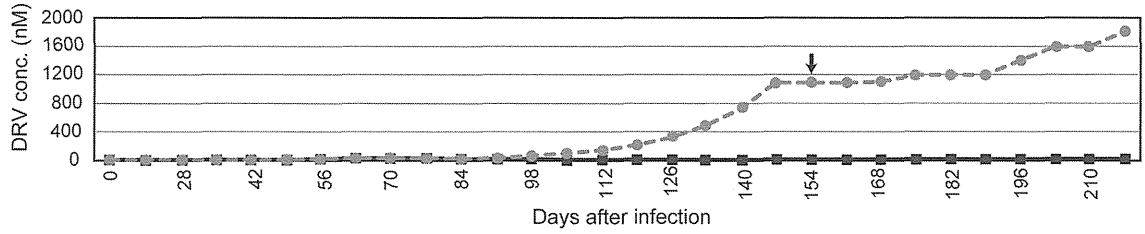


**FIGURE 2 | *In vitro* selection to induce DRV-resistant viruses.** The selection of FS5929 and HIV-1 JR-CSF are indicated with gray dotted and black solid lines, respectively. The arrow indicates the sampling time point for the collection of FS5929R, which we focused on in this study. The x-axis and y-axis represent "days after the initial viral infection to cell culture" and "DRV concentration (μM) in cell culture medium," respectively.

**TABLE 3 | Gag sequence of major DRV-resistant viruses.**

| Positions* | | 10 | 20 | 30 | 40 | 50 | 60 |
|---|---|---|---|---|---|---|---|
| NL4-3 | | MGARASVLSG | GELDKWEKIR | LRPGGKKQYK | LKHIVWASRE | LERFAVNPGL | LETSEGCRQI |
| FS5929 | (Day 0) | ---------- | ---------- | -------K-R | ---------- | ---------- | ---------- |
| FS5929R | (Day 154)† | ---------- | -K-------- | -------K-R | ---------- | ---------- | ---------- |
| Positions | | 70 | 80 | 90 | 100 | 110 | 120 |
| NL4-3 | | LGQLQPSLQT | GSEELRSLYN | TIAVLYCVHQ | RIDVKDTKEA | LDKIEEEQNK | SKKKAQQAAA |
| FS5929 | (Day 0) | ---------- | ---------- | ---T------ | ---------- | -E-------- | ---------- |
| FS5929R | (Day 154) | ---------- | ---------- | ---T------ | ---------- | -E-------- | ---------- |
| Positions | | 129 | 139 | 149 | 159 | 169 | 179 |
| | | X | XXXXXXX | | | | |
| NL4-3 | | DTGNNS QVS | QNYPIVQNLQ | GQMVHQAISP | RTLNAWVKVV | EEKAFSPEVI | PMFSALSEGA |
| FS5929 | (Day 0) | ------SK-- | --F------- | ---------- | ---------I | ---------- | ---------- |
| FS5929R | (Day 154) | ------SK-- | --F------- | ---------- | ---------I | ---------- | ---------- |
| Positions | | 189 | 199 | 209 | 219 | 229 | 239 |
| NL4-3 | | TPQDLNTMLN | TVGGHQAAMQ | MLKETINEEA | AEWDRLHPVH | AGPIAPGQMR | EPRGSDIAGT |
| FS5929 | (Day 0) | ---------- | ---------- | ---------- | --------P Q | ---------- | ---------A |
| FS5929R | (Day 154) | ---------- | ---------- | ---------- | --------P Q | ---------- | ---------A |
| Positions | | 249 | 259 | 269 | 279 | 289 | 299 |
| NL4-3 | | TSTLQEQIGW | MTHNPPIPVG | EIYKRWIILG | LNKIVRMYSP | TSILDIRQGP | KEPFRDYVDR |
| FS5929 | (Day 0) | ---------- | --S---V--- | ---------- | ---------- | V--------- | ---------- |
| FS5929R | (Day 154) | ---------- | --N------- | ---------- | ---------- | V--------- | ---------- |
| Positions | | 309 | 319 | 329 | 339 | 349 | 359 |
| NL4-3 | | FYKTLRAEQA | SQEVKNWMTE | TLLVQNANPD | CKTILKALGP | GATLEEMMTA | CQGVGGPGHK |
| FS5929 | (Day 0) | ---------- | ---------- | ---------- | ---------- | A--------- | ---------- |
| FS5929R | (Day 154) | ---------- | ---------- | ---------- | ---------- | A--------- | ---------- |
| Positions | | 369 | 379 | 389 | 399 | 409 | 419 |
| | | XXXXXXXX | XXXXXX | XX | | | |
| NL4-3 | | ARVLAEAMSQ | VTNPATIMIQ | KGNFRNQRKT | VKCFNCGKEG | HIAKNCRAPR | KKGCWKCGKE |
| FS5929 | (Day 0) | ---------L | --H-----M- | ------P--- | ---------- | -V-R------ | -R-------- |
| FS5929R | (Day 154) | ---------L | --H-----M- | ------P--- | ---------- | -V-R------ | ---------- |
| Positions | | 429 | 439 | 449 | 458 | 456 | 466 |
| | | X | XXXXXXX | XXXXXX | XX | | |
| NL4-3 | | GHQMKDCTER | QANFLGKIWP | SHKGRPGNFL | QSRPEPTAP | PEESFRFG | EETTTPSQKQ |
| FS5929 | (Day 0) | -------A-- | -IH--E---- | ---------- | ---A-----P | AP-------- | ---------- |
| FS5929R | (Day 154) | ---------- | -IH--E---- | ---------- | ---A-----P | AP-------- | -K-------- |
| Positions | | 476 | | | | | |
| NL4-3 | | EPIDKELYPL | A | | | | |
| FS5929 | (Day 0) | --M-EG---- | - | | | | |
| FS5929R | (Day 154) | ----EG---- | - | | | | |

*FS5929 and FS5929R denote the input viruses for the in vitro selection (day 0) and the virus mixture obtained at the day 154, respectively.*
**The eight residues flanking at each of five PR cleavage sites in Gag (MA-CA, CA-p2, p2-NC, NC-p1, and p1-p6) were highlighted with "X."*
*†The Gag sequence was shown as a major population sequence.*

**TABLE 4 | PI susceptibility assays of recombinant viruses.**

| | NL4-3 | rFS5929 | rFS5929R1 | rFS5929R1$_{I47}$ | rFS5929R1$_{I50}$ | rFS5929R1$_{I47/I50}$ |
|---|---|---|---|---|---|---|
| DRV | 0.0057 ± 0.0006* | 0.0111 ± 0.0036 (1.9†) | >1 (>175.3) | >1 (>175.3) | 0.5528 ± 0.0722 (96.9) | 0.1162 ± 0.0149 (20.4) |
| APV | 0.0278 ± 0.0042 | 0.4440 ± 0.1263 (16.0) | >1 (>35.9) | >1 (>35.9) | >1 (>35.9) | >1 (>35.9) |
| LPV | 0.0182 ± 0.0011 | >1 (>54.9) | >1 (>54.9) | >1 (>54.9) | >1 (>54.9) | 0.9493 ± 0.0453 (52.1) |
| RTV | 0.0347 ± 0.0049 | >1 (>28.8) | >1 (>28.8) | >1 (>28.8) | >1 (>28.8) | >1 (28.8) |
| NFV | 0.0120 ± 0.0006 | >1 (>83.1) | >1 (>83.1) | >1 (>83.1) | >1 (>83.1) | >1 (>83.1) |
| TPV | 0.1368 ± 0.0119 | 0.0646 ± 0.0192 (0.5) | 0.0500 ± 0.0119 (0.4) | 0.0204 ± 0.0068 (0.1) | 0.2397 ± 0.0250 (1.8) | 0.1810 ± 0.0037 (1.3) |
| ATV | 0.0047 ± 0.0013 | 0.0481 ± 0.0129 (10.2) | 0.0178 ± 0.0039 (3.8) | 0.0490 ± 0.0109 (10.4) | 0.0489 ± 0.0143 (10.4) | 0.1350 ± 0.0236 (28.7) |
| SQV | 0.0203 ± 0.0077 | 0.3030 ± 0.0622 (14.9) | 0.2500 ± 0.0506 (12.3) | 0.2631 ± 0.0555 (13.0) | 0.1838 ± 0.0451 (9.1) | 0.2440 ± 0.0183 (12.0) |

*$IC_{50}$ ($\mu$M).
†*Fold changes from $IC_{50}$ of HIV-1 NL4-3 are written in parentheses.*

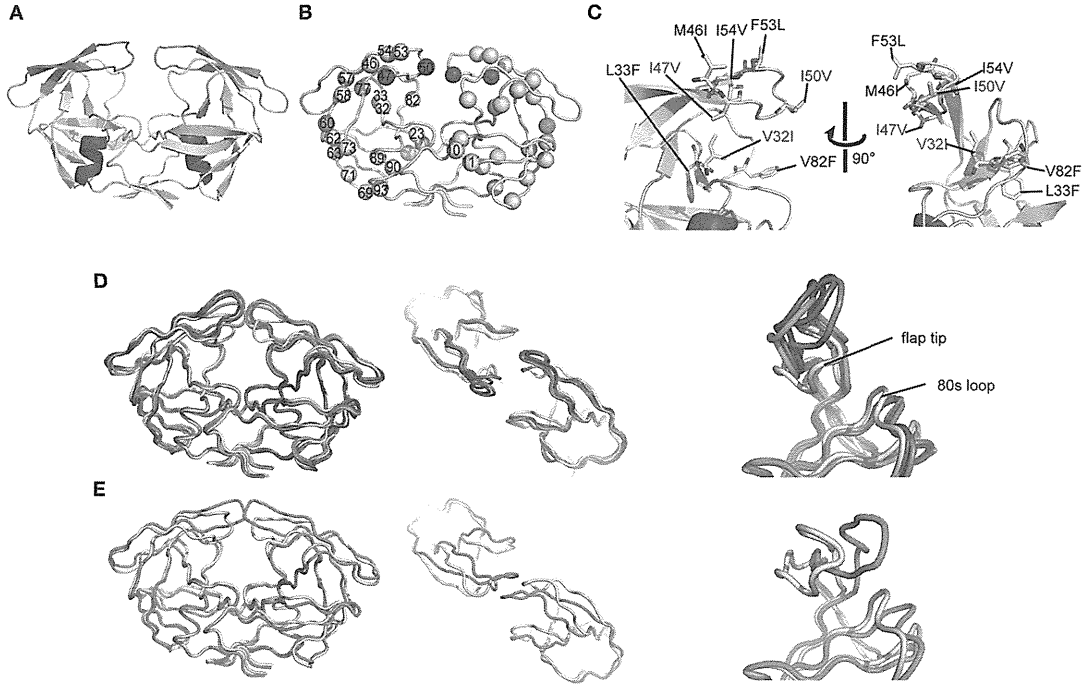


**FIGURE 3 | Crystal structure of FS5929R1 PR. (A)** Ribbon diagram of the PR, which forms a homodimer. The α-helices and β-strands are colored in red and yellow, respectively. The flap regions (residues 43–58) are highlighted in orange. **(B)** Locations of mutated residues on the PR. The red, yellow, and green spheres indicate the locations of the major DRV resistance, minor DRV resistance, and other mutations, respectively, that appeared after the DRV-resistance induction experiment using FS5929. Mutations that originally existed in FS5929 are shown in gray spheres. **(C)** Highlighted structure around the flaps in the PR. The mutations are shown as sticks. The mutations V32I, I47V, and I50V, which appeared during the *in vitro* selection, are highlighted with red letters. **(D)** Superposition of our crystal structures of the PRs (gray) with the crystal structures of the open form [PDB IDs: 2PC0 (cyan), 1TW7 (purple), 4NPU (orange), and 3UF3 (navy)]. **(E)** Superposition of our crystal structures of the PRs with a crystal structure of the semi-open form [PDB IDs: 1HHP (green)].

to DRV from a clinically isolated multiple drug-resistant sample (FS5929). FS5929 contained one minor DRV resistance mutation (L33F) (**Table 2**) and conferred the highest DRV resistance (7.7-fold increase compared with the WT HIV-1 JR-CSF) of the 20 multiple drug-resistant samples selected for this study (**Figure 1** and **Table 1**). After 154 days of culture in the presence of increasing concentrations of DRV, we obtained a virus mixture (FS5929R) with high-level resistance to DRV that was viable in cultures with 1000 nM DRV (**Figure 2**). Population sequence analyses of the PR region indicated that FS5929R consisted of at least seven variants (**Table 2**). The major virus (referred to as FS5929R1) had two major DRV resistance mutations (I47V and I50V), four minor mutations (V11I, V32I, L33F, and L89V), and V82F. The other minor variants had I47V mutation and either of I50V or L76V mutation although the other sequences were similar to that of the major virus. Additionally, we examined the PR cleavage sites in the *gag* sequences. No sequence changes around the cleavage sites occurred during culture (**Table 3**), although mutations at the flanking regions of the cleavage sites were observed in both FS5929 and FS5929R1 (except for the

**TABLE 5 | Crystallographic data collection and refinement statistics.**

| Parameter | Value(s) for HIV-1 PR |
|---|---|
| **DATA COLLECTION** | |
| Space group | *P*1 |
| Unit cell dimensions | |
| *a* (Å) | 37.1 |
| *b* (Å) | 48.7 |
| *c* (Å) | 54.2 |
| $\alpha$ (degree) | 89.9 |
| $\beta$ (degree) | 74.0 |
| $\gamma$ (degree) | 86.7 |
| Wave length (Å) | 1.0 |
| Resolution (Å) | 50–1.80 (1.86–1.80) |
| $R_{merge}$ (%) | 4.4 (19.4) |
| Average $I/\sigma$ (I) | 26.9 (3.7) |
| Completeness (%) | 96.0 (92.7) |
| Multiplicity | 1.9 (1.9) |
| **REFINEMENT** | |
| Unique reflections | 30928 |
| $R_{work}$ (%)/$R_{free}$ (%) | 19.6/24.0 |
| No. of non-H atoms | |
| Protein | 3174 |
| Chloride ion | 5 |
| Water molecules | 142 |
| RMS deviation from ideality | |
| Bonds (Å) | 0.019 |
| Angle distance (degree) | 2.06 |
| Ramachandran plot | |
| Preferred region (%) | 95.2 |
| Allowed region (%) | 4.0 |
| Outlier regions (%) | 0.8 |
| Average B-factors (Å$^2$) | |
| Main chain | 25.3 |
| Side chain | 28.0 |
| Solvent | 33.9 |

*Values in parentheses correspond to the highest resolution shell. The structure has been deposited as 5B18 in Protein Data Bank (PDB).*

sites between the capsid and p2 and between p1 and p6). Together, these results show that the high-level DRV resistance of FS5929R is mainly attributed to the accumulation of DRV resistance-associated mutations in the PR region. In contrast, no DRV-resistant virus was developed by the induction of the WT HIV-1 JR-CSF for over half of a year (**Figure 2**) as detailed in previous reports (De Meyer et al., 2005; Surleraux et al., 2005; Dierynck et al., 2007).

## The Major PR Obtained from *in vitro* Selection is Resistant to DRV but Not to TPV

Next, we focused on FS5929R1 and analyzed its resistance to DRV. We generated recombinant viruses carrying the *gag-PR* of FS5929R1 (rFS5929R1) and FS5929 (rFS5929) based on the HIV-1 NL4-3 backbone. The susceptibility assays showed that rFS5929R1 displayed a >175-fold increase in DRV resistance compared with that of WT NL4-3, whereas FS5929 was susceptible to DRV (1.9-fold increase) (**Table 4**). We also constructed three recombinant rFS5929R1 viruses lacking the major DRV resistance mutations I47V and/or I50V to assess the contribution of the major mutations to DRV resistance. Each rFS5929R1 virus without I47V (rFS5929R1$_{I47}$) and rFS5929R1 without I50V (rFS5929R1$_{I50}$) exhibited a >175-fold and 96.9-fold increase in DRV resistance, respectively, whereas the rFS5929R1 without the two mutations (rFS5929R1$_{I47/I50}$) exhibited a 20.4-fold increase. The results suggest that the two major mutations, especially I50V, largely contribute to the DRV resistance in rFS5929R1.

We also measured the resistance to seven other PIs: amprenavir (APV), lopinavir (LPV), ritonavir (RTV), nelfinavir (NFV), tipranavir (TPV), atazanavir (ATV), and saquinavir (SQV). The rFS5929 and rFS5929R1 viruses exhibited 16.0- and >35.9-fold resistance, respectively, to the DRV-analog APV. Both viruses exhibited high-level resistance to LPV (>54.9 fold), RTV (>28.8 fold), and NFV (>83.1 fold). Interestingly, both viruses were susceptible to TPV (<0.5 fold) and exhibited 3- to 15-fold resistance to ATV and SQV, suggesting that the mutations induced by the *in vitro* selection with DRV scarcely affected the susceptibilities to TPV, ATV, and SQV.

## Determination of the High-Resolution Crystal Structure of the Ligand-Free State of FS5929R1 PR

To investigate the mechanism underlying the DRV resistance of FS5929R1, we determined the crystal structure of the ligand-free state of the inactive FS5929R1 PR homodimer at a 1.8 Å resolution (**Figure 3** and **Table 5**). Our crystal structure had a conformation similar to that of the open forms (**Figure 3D**), as seen in the previous crystal structures of ligand-free PRs (PDB IDs: 2PC0, 1TW7, 4NPU, and 3UF3; Martin et al., 2005; Heaslet et al., 2007; Agniswamy et al., 2012; Zhang et al., 2014). Although two additional PR conformations have been reported [a semi-open form favored by the ligand-free state of the WT PR (PDB ID: 1HHP) (Spinelli et al., 1991; Hornak et al., 2006b; Deng et al., 2011) and a closed form favored by the ligand-bound state of PR (e.g., PDB ID: 1HVR) (Lam et al., 1994)], few contacts existed between the flap regions of the two monomers in our structure, which was in contrast to these semi-open or closed forms. The root mean squared deviation (RMSD) values of all Cα atoms in our crystal structure compared with those in the open-form structures (2PC0, 1TW7, 4NPU, and 3UF3) were 1.36, 1.42, 1.42, and 1.33 Å, respectively (**Figure 4**). Contrastingly, the crystal structures of the semi-open and closed forms (1HHP and 1HVR) showed higher RMSD values (1.62 and 1.76 Å) than for the open-form structures (**Figure 3E**). Notably, two of the open-form structures (4NPU and 3UF3) were the previously reported crystal structures of other PRs with high-level resistance to DRV, suggesting that PRs with high-level resistance to DRV commonly favor configurations that resemble the open form.

**A**

RMSD (Å)

| | 1HVR | 1HHP | 2PC0 | 1TW7 | 4NPU | 3UF3 |
|---|---|---|---|---|---|---|
| 1HVR | | | | | | |
| 1HHP | 1.88 | | | | | |
| 2PC0 | 2.30 | 1.83 | | | | |
| 1TW7 | 2.03 | 1.68 | 0.68 | | | |
| 4NPU | 2.10 | 1.49 | 0.86 | 0.85 | | |
| 3UF3 | 2.35 | 1.84 | 0.63 | 0.90 | 0.85 | |
| This study | 1.76 | 1.62 | 1.36 | 1.42 | 1.42 | 1.33 |

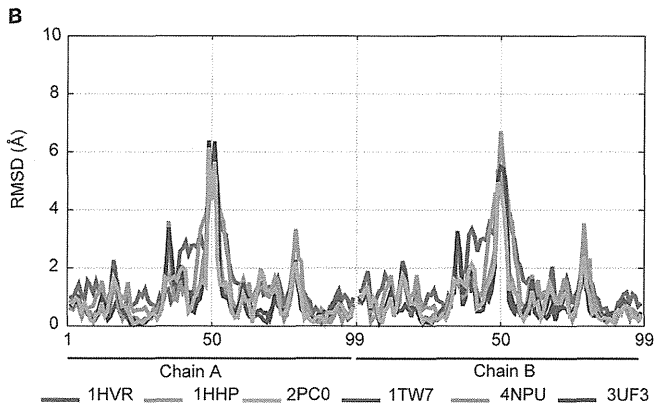


**FIGURE 4 | Comparison of the crystal structures of ligand-free PRs; closed-form (PDB ID: 1HVR), semi-open form (1HHP), open form (2PC0, 1TW7, 4NPU, and 3UF3), and the PR purified in this study. (A)** RMSD calculations comparing the crystal structures by using the coordinates of the Cα atoms. **(B)** Comparison of each Cα atom in the PR structures with the corresponding Cα atom in the FS5929R1 PR.

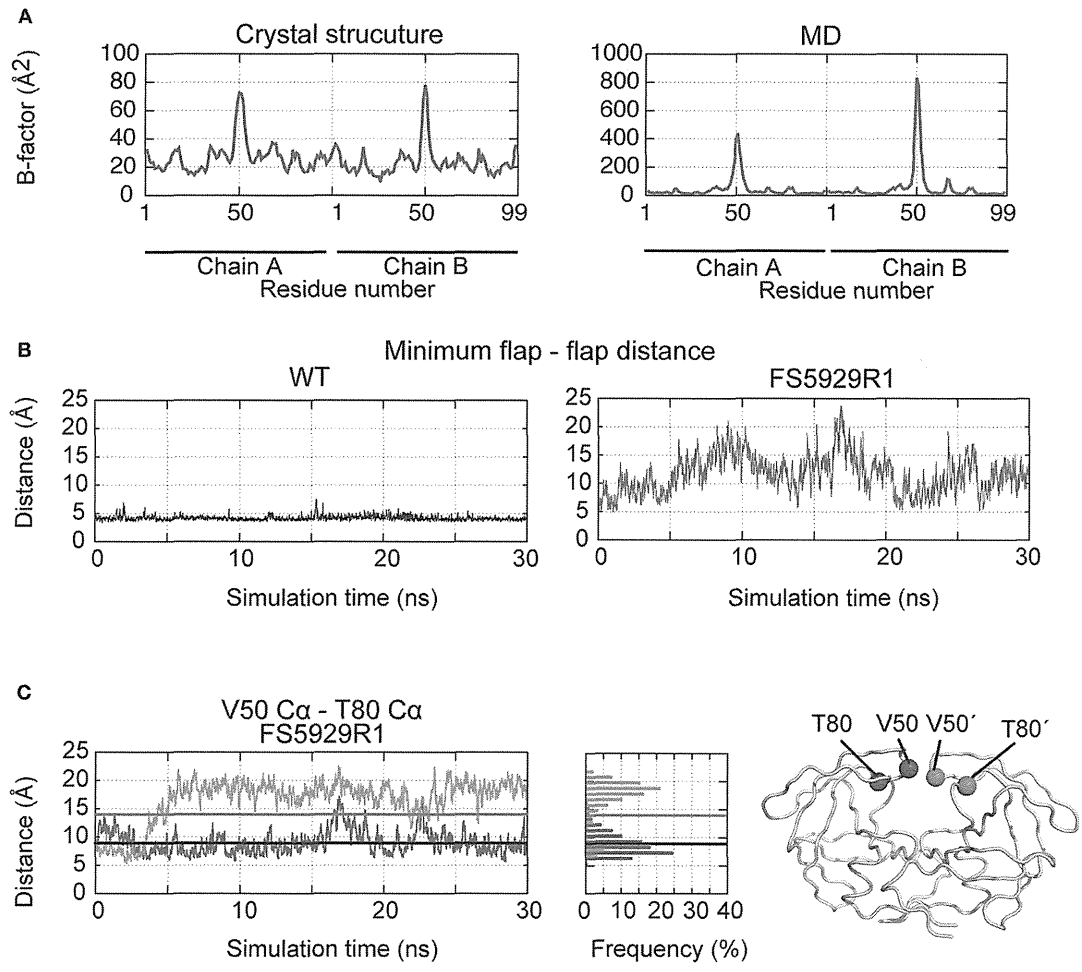


**FIGURE 5 | Flap dynamics in the crystal structure and MD simulations. (A)** B factors of the respective residues in the FS5929R1 PR estimated from the crystal structure and MD simulations. **(B)** The minimum distance between two flaps in the WT and FS5929R1 PRs calculated with an in-house program. **(C)** The time course of the distance between the V50 Cα and the T80 Cα (left, red) or between the V50′ Cα and the T80′ Cα (left, green) and their histogram (center). The black and gray solid lines indicate the distances in the crystal structure from our study and an open-form structure (PDB ID: 3UF3), respectively. The structural positions of the V50 and T80 Cαs (red) in one monomer and the V50′ and T80′ Cαs in a second monomer are highlighted on the right side of the figure of the PR structure.

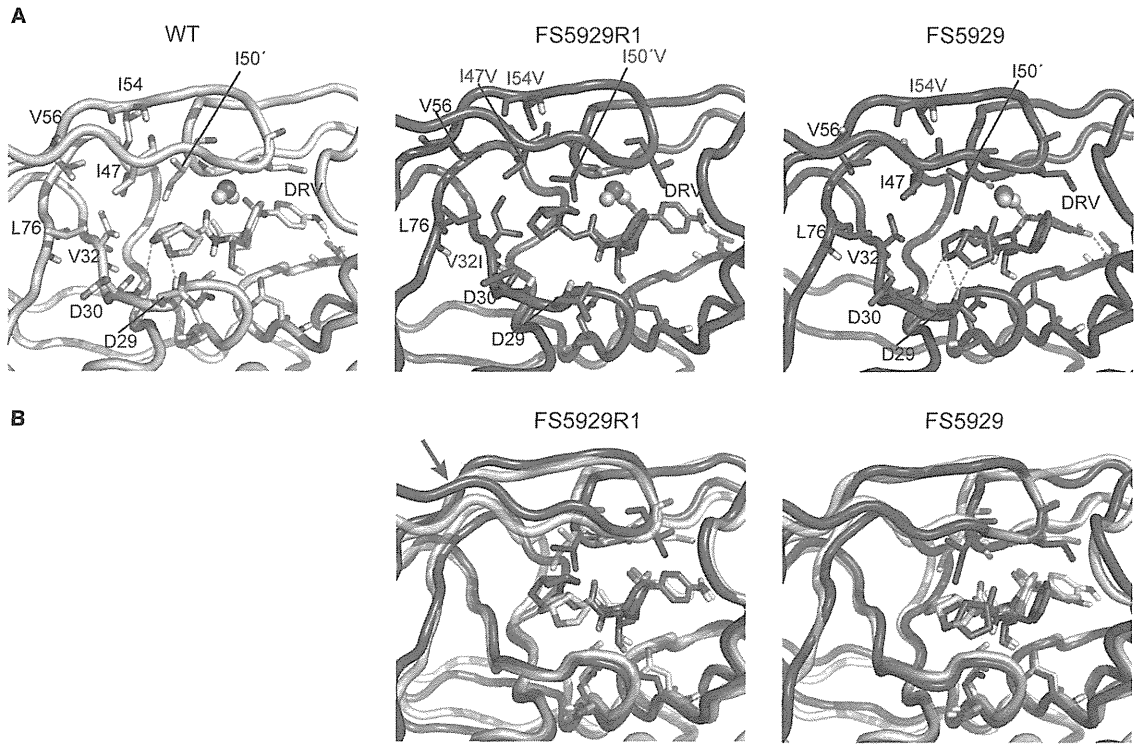


**FIGURE 6 | Representative structures of simulations of each PR with DRV. (A)** Interactions between PR and DRV. The orange dotted lines indicate hydrogen bonds. **(B)** Superposition onto the WT PR structure. Stick representations show important residues in WT (gray), FS5929R1 (purple), and FS5929 PR (blue) structures. The red arrow indicates the flap region shifted outward in the FS5929R1 PR with DRV.

Our crystal structure had a distinct conformation at the flap regions and the 80s loops that was absent in the open-form structures. The flap tip that are around the 50th residue curled inward in our crystal structure, whereas the 80s loops were slightly shifted inside of the PR. Therefore, the flap tips approached the 80s loop within the same monomer. The distance between the Cα atoms of the 50th and 80th residues within the same monomer of our crystal structure was approximately 8.9 Å, whereas the distances were approximately 14.1 and 14.0 Å in the open-form crystal structures (4NPU and 3UF3, respectively). Interestingly, the regions included the two major DRV resistance mutations (I47V and I50V) and one minor mutation (V32I), which were induced by the *in vitro* selection (**Figure 3C**). Hence, the unique curling structure at the flap regions was likely associated with the DRV resistance of FS5929R1.

To assess the stability of the unique curling conformation at the mobile flap regions of the FS5929R1 PR (**Figure 5A**), we performed 30.0 ns-timescale MD simulations using the determined structure as the initial structure. The MD simulations suggested that the FS5929R1 PR favored conformations in which the flaps in each monomer were separated, which was in contrast to the WT PR (**Figure 5B** and **Supplemental Movies S1**, **S2**). Furthermore, constant curling at the flap region was observed in one monomer but not the second monomer (**Figure 5C**). These observations suggested that the flap in at least one monomer would frequently adopt the curling conformation despite the high mobility of the flap.

## Structure Prediction of the FS5929R1 PR in Complex with DRV

Finally, to evaluate the binding mode of DRV to the FS5929R and FS5929R1 PRs, we predicted the interactions of both PRs with DRV, from a crystal structure of the WT PR in complex with DRV, by MD simulations (**Figure 6**) as described in our previous reports (Ode et al., 2007a,b). The MD simulations indicated that a flap region of FS5929R1 PR in complex with DRV shifts outward compared with that of the WT PR in complex with DRV; this change was not observed in FS5929 PR in complex with DRV. Furthermore, the FS5929R1 PR could not create direct hydrogen bonds with the DRV *bis*-tetrahydrofuran (*bis*-THF) moiety and the central hydroxyl group (**Figure 7**). In contrast, FS5929 PR could create hydrogen bonds with DRV that were similar to those of the WT PR despite slight differences in the PR-DRV hydrogen bond networks between the WT and FS5929 PRs. The binding energy calculations indicated a 10.9 kcal $mol^{-1}$ loss of the binding energy with DRV for each FS5929R1 PR and a 0.8 kcal $mol^{-1}$ loss for FS5929 PR compared with the WT PR in complex with DRV. These results were consistent with the DRV susceptibility results shown in **Table 4**, suggesting that the conformational change in the flap likely affected the binding of DRV to PR.

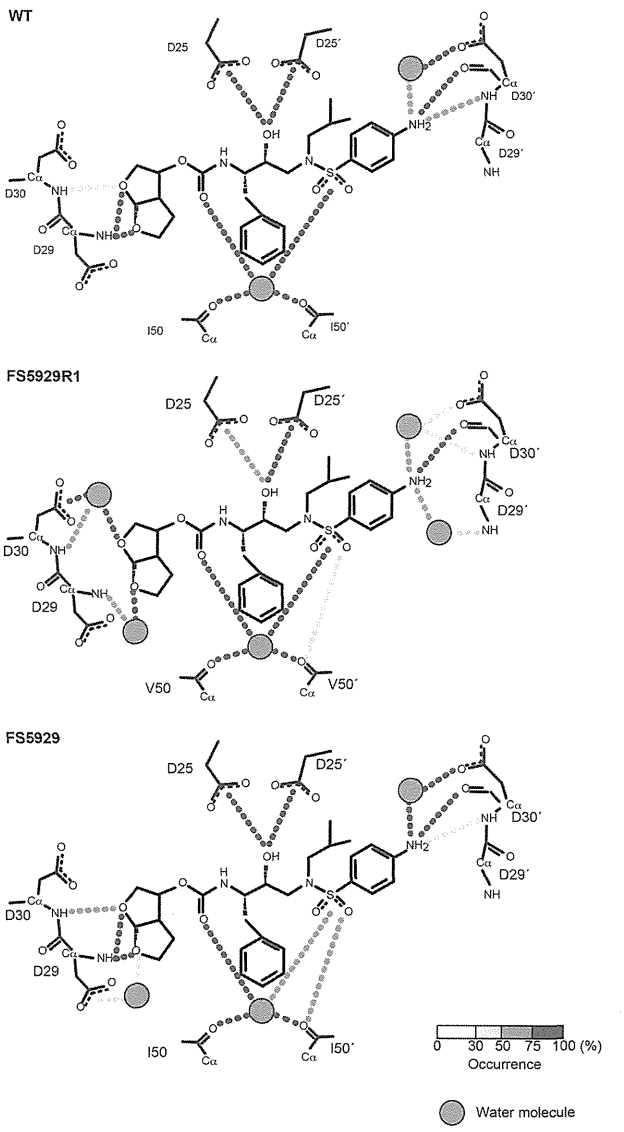


**FIGURE 7 | Hydrogen bond network between PR and DRV predicted from MD simulations.** The residues in PR and DRV are highlighted with blue and black, respectively. Hydrogen bonds are represented by dotted lines colored according to their occurrence during the 5.0–6.0 ns simulations, as shown in the bottom bar.

## DISCUSSION

The virus with high-level resistance to DRV that was generated in this study (referred to as FS5929R1) harbored 6 DRV resistance-associated mutations in its PR region. The drug susceptibility tests with the recombinant virus variants suggested that the *in vitro* selection specifically increased the resistance to DRV and its structural analog APV (**Table 4**). The two major mutations (especially I50V) greatly contributed to the resistance of the PR, which was in agreement with the effects of single substitutions on the binding of DRV to the WT PR (De Meyer et al., 2006; Tremblay, 2008).

Notably, the crystal structure of the ligand-free FS5929R1 PR showed an open-form configuration that was similar to those of the two previously reported ligand-free structures of PRs with high-level resistance to DRV (PDB IDs: 4NPU and 3UF3). However, the FS5929R1 PR exhibited a unique curling conformation at the flaps (**Figure 3**). Because the FS5929R1 PR harbored the major mutation I50V, which was absent in the other two PRs, the unique flap conformation is likely attributable to I50V. The curled flap conformations in the FS5929R1 PR might hinder the DRV access to the active site of dimeric PR because the flap tips tended to curl toward the active site. Furthermore, the unique flap conformation of the FS5929R1 PR would influence DRV resistance through the change in flexibility of the flap in the dimeric PR suggested by our MD simulations (**Figure 5**) and proposed in previous MD and NMR studies of other PI-resistant mutants (Perryman et al., 2004; Cai et al., 2012). The high mobility of the flaps of the FS5929R1 PR would provide little opportunity for the formation of PI-binding pockets, resulting in reduced opportunity to bind to DRV. Moreover, when the PR binds DRV, the high flap mobility coupled with effects of active site mutations, such as V32I, I47V, and I50V (Kovalevsky et al., 2006; Liu et al., 2008; Mittal et al., 2013), may result in instability of the complex due to the expansion of the PI-binding pocket (Cai et al., 2014; **Figure 6**).

It is also plausible that the preference for the unique conformation in FS5929R1 PR would reduce the PR dimerization inhibition activity of DRV, which is the second inhibitory mechanism of DRV (Koh et al., 2007, 2011). DRV appears to bind the region around the 32nd, 33rd, 54th, and 82nd residues in monomeric PR (Koh et al., 2011; Huang and Caflisch, 2012; Hayashi et al., 2014). These four residues are positioned close to the flap tips on the FS5929R1 PR structure. Therefore, the curling conformation would also shield these residues, resulting in the inhibition of DRV binding to monomeric PR; in contrast, the presence of four mutations (V32I, L33F, I54V, and V82F) in FS5929R1 PR might directly impair the DRV binding to monomeric PR.

The DRV-resistant FS5929R1 PR remained susceptible to TPV and exhibited low-to-intermediate resistance to ATV and SQV, which was similar to the results of previous reports on distinct DRV-resistant viruses (Dierynck et al., 2007; Saskova et al., 2009; Rhee et al., 2010). Furthermore, the DRV resistance mutation I50V was related to hypersusceptibility to TPV (Schapiro et al., 2010; Bethell et al., 2012), whereas I50V had the potential to increase susceptibility to ATV (Mittal et al., 2013). Together with our structural information, this information suggests that the distinct susceptibilities might be attributed to the strength of the interactions between the flaps in the PR and these PIs. Crystal structures of the WT PR with TPV, ATV, and SQV (PDB IDs: 1D4Y, 2AQU, and 1HXB, respectively) (Krohn et al., 1991; Thaisrivongs et al., 1996; Clemente et al., 2006) indicate that these PIs commonly have strong interactions with the flaps, which differ from the other PIs. TPV has direct interactions with the main chains of I50 in the flaps, whereas the bulky aromatic rings in ATV and SQV largely interact with the flaps. DRV creates water molecule-mediated hydrogen bonds with the flaps. Therefore, the conformational changes at the flaps may scarcely

affect the binding of TPV, ATV, and SQV but not DRV. Obtaining information on the interactions between PR and PIs will aid in the development of PIs that are more potent than DRV against PRs with accumulated mutations at the flap.

In conclusion, we identified a novel structural feature that influences DRV resistance via *in vitro* selection of HIV-1 variants with high-level resistance to DRV and subsequent determination of a crystal structure and a MD simulation of its PR. The information will aid in the development of potent PIs against DRV-resistant viruses.

## ACCESSION NUMBER

Coordinates and structure factors have been deposited into the Protein Data Bank (PDB) with the accession code 5B18.

## AUTHOR CONTRIBUTIONS

Conceived and designed the experiments: WS and YI. Performed the experiments: MN, HO, KS, MF, MMaejima, YK, TM, JH, MMatsuda, AH, and YI. Analyzed the data: MN, HO, KS, MF, MMaejima, and YI. Contributed reagents/materials/analysis tools: YY, AS, NW, WS, and YI. Wrote the paper: MN, HO, and YI.

## FUNDING

This study was supported by the Japan Society for the Promotion of Science (JSPS) fellows (MN) under grant number 15J12567, by the JSPS (YI) under grant number 15H04740, and by the Japan Agency for Medical Research and Development (AMED) (YI and NW).

## ACKNOWLEDGMENTS

The synchrotron radiation experiments were performed at the BL38B1 of SPring-8 with the approval of the Japan Synchrotron Radiation Research Institute (JASRI) (Proposal No. 2011B1255).

## SUPPLEMENTARY MATERIAL

The Supplementary Material for this article can be found online at: http://journal.frontiersin.org/article/10.3389/fmicb.2016.00061

**Supplemental Movie S1 | Flap dynamics in WT PR at ligand-free states.**

**Supplemental Movie S2 | Flap dynamics in FS5929R1 PR at ligand-free states.**

## REFERENCES

Agniswamy, J., Shen, C. H., Aniana, A., Sayer, J. M., Louis, J. M., and Weber, I. T. (2012). HIV-1 protease with 20 mutations exhibits extreme resistance to clinical inhibitors through coordinated structural rearrangements. *Biochemistry* 51, 2819–2828. doi: 10.1021/bi2018317

Bethell, R., Scherer, J., Witvrouw, M., Paquet, A., Coakley, E., and Hall, D. (2012). Short communication: phenotypic protease inhibitor resistance and cross-resistance in the clinic from 2006 to 2008 and mutational prevalences in HIV from patients with discordant tipranavir and darunavir susceptibility phenotypes. *AIDS Res. Hum. Retrovirus.* 28, 1019–1024. doi: 10.1089/AID.2011.0242

Cai, Y., Myint, W., Paulsen, J. L., Schiffer, C. A., Ishima, R., and Kurt Yilmaz, N. (2014). Drug resistance mutations alter dynamics of inhibitor-bound HIV-1 protease. *J. Chem. Theory Comput.* 10, 3438–3448. doi: 10.1021/ct4010454

Cai, Y., Yilmaz, N. K., Myint, W., Ishima, R., and Schiffer, C. A. (2012). Differential flap dynamics in wild-type and a drug resistant variant of HIV-1 protease revealed by molecular dynamics and NMR relaxation. *J. Chem. Theory Comput.* 8, 3452–3462. doi: 10.1021/ct300076y

Case, D. A., Darden, T. A., Cheatham, T. E. I., Simmerling, C. L., Wang, J., Duke, R. E., et al. (2006). *AMBER 9*. San Francisco, CA: University of California.

Chiba-Mizutani, T., Miura, H., Matsuda, M., Matsuda, Z., Yokomaku, Y., Miyauchi, K., et al. (2007). Use of new T-cell-based cell lines expressing two luciferase reporters for accurately evaluating susceptibility to anti-human immunodeficiency virus type 1 drugs. *J. Clin. Microbiol.* 45, 477–487. doi: 10.1128/JCM.01708-06

Clemente, J. C., Coman, R. M., Thiaville, M. M., Janka, L. K., Jeung, J. A., Nukoolkarn, S., et al. (2006). Analysis of HIV-1 CRF_01 A/E protease inhibitor resistance: structural determinants for maintaining sensitivity and developing resistance to atazanavir. *Biochemistry* 45, 5468–5477. doi: 10.1021/bi051886s

Delaugerre, C., Pavie, J., Palmer, P., Ghosn, J., Blanche, S., Roudiere, L., et al. (2008). Pattern and impact of emerging resistance mutations in treatment experienced patients failing darunavir-containing regimen. *AIDS* 22, 1809–1813. doi: 10.1097/QAD.0b013e328307f24a

De Meyer, S., Azijn, H., Surleraux, D., Jochmans, D., Tahri, A., Pauwels, R., et al. (2005). TMC114, a novel human immunodeficiency virus type 1 protease inhibitor active against protease inhibitor-resistant viruses, including a broad range of clinical isolates. *Antimicrob. Agents Chemother.* 49, 2314–2321. doi: 10.1128/AAC.49.6.2314-2321.2005

De Meyer, S., Lefebvre, E., Azjin, H., de Baere, I., van Baelen, B., and de Bethune, M. P. (2006). "Phenotypic and genotypic determinants of resistance to TMC 114: pooled analysis of POWER 1, 2 and 3," in *15th International HIV Drug Resistance Workshop* (Sitges).

Deng, N. J., Zheng, W., Gallicchio, E., and Levy, R. M. (2011). Insights into the dynamics of HIV-1 protease: a kinetic network model constructed from atomistic simulations. *J. Am. Chem. Soc.* 133, 9387–9394. doi: 10.1021/ja2008032

Dierynck, I., de Wit, M., Gustin, E., Keuleers, I., Vandersmissen, J., Hallenberger, S., et al. (2007). Binding kinetics of darunavir to human immunodeficiency virus type 1 protease explain the potent antiviral activity and high genetic barrier. *J. Virol.* 81, 13845–13851. doi: 10.1128/JVI.01184-07

Dierynck, I., van Marck, H., van Ginderen, M., Jonckers, T. H., Nalam, M. N., Schiffer, C. A., et al. (2011). TMC310911, a novel human immunodeficiency virus type 1 protease inhibitor, shows *in vitro* an improved resistance profile and higher genetic barrier to resistance compared with current protease inhibitors. *Antimicrob. Agents Chemother.* 55, 5723–5731. doi: 10.1128/AAC.00748-11

Emsley, P., Lohkamp, B., Scott, W. G., and Cowtan, K. (2010). Features and development of Coot. *Acta Crystallogr. D Biol. Crystallogr.* 66, 486–501. doi: 10.1107/S0907444910007493

Ghosh, A. K., Sridhar, P. R., Leshchenko, S., Hussain, A. K., Li, J., Kovalevsky, A. Y., et al. (2006). Structure-based design of novel HIV-1 protease inhibitors to combat drug resistance. *J. Med. Chem.* 49, 5252–5261. doi: 10.1021/jm060561m

Hattori, J., Shiino, T., Gatanaga, H., Yoshida, S., Watanabe, D., Minami, R., et al. (2010). Trends in transmitted drug-resistant HIV-1 and demographic characteristics of newly diagnosed patients: nationwide surveillance from 2003 to 2008 in Japan. *Antiviral Res.* 88, 72–79. doi: 10.1016/j.antiviral.2010.07.008

Hayashi, H., Takamune, N., Nirasawa, T., Aoki, M., Morishita, Y., Das, D., et al. (2014). Dimerization of HIV-1 protease occurs through two steps relating to the mechanism of protease dimerization inhibition by darunavir. *Proc. Natl. Acad. Sci. U.S.A.* 111, 12234–12239. doi: 10.1073/pnas.1400027111

Heaslet, H., Rosenfeld, R., Giffin, M., Lin, Y. C., Tam, K., Torbett, B. E., et al. (2007). Conformational flexibility in the flap domains of ligand-free HIV protease. *Acta Crystallogr. D Biol. Crystallogr.* 63, 866–875. doi: 10.1107/S0907444907029125

Hornak, V., Abel, R., Okur, A., Strockbine, B., Roitberg, A., and Simmerling, C. (2006a). Comparison of multiple Amber force fields and development of improved protein backbone parameters. *Proteins* 65, 712–725. doi: 10.1002/prot.21123

Hornak, V., Okur, A., Rizzo, R. C., and Simmerling, C. (2006b). HIV-1 protease flaps spontaneously open and reclose in molecular dynamics simulations. *Proc. Natl. Acad. Sci. U.S.A.* 103, 915–920. doi: 10.1073/pnas.0508452103

Huang, D., and Caflisch, A. (2012). How does darunavir prevent HIV-1 protease dimerization? *J. Chem. Theory Comput.* 8, 1786–1794. doi: 10.1021/ct300032r

King, N. M., Melnick, L., Prabu-Jeyabalan, M., Nalivaika, E. A., Yang, S. S., Gao, Y., et al. (2002). Lack of synergy for inhibitors targeting a multi-drug-resistant HIV-1 protease. *Protein Sci.* 11, 418–429. doi: 10.1110/ps.25502

Koh, Y., Amano, M., Towata, T., Danish, M., Leshchenko-Yashchuk, S., Das, D., et al. (2010). *In vitro* selection of highly darunavir-resistant and replication-competent HIV-1 variants by using a mixture of clinical HIV-1 isolates resistant to multiple conventional protease inhibitors. *J. Virol.* 84, 11961–11969. doi: 10.1128/JVI.00967-10

Koh, Y., Aoki, M., Danish, M. L., Aoki-Ogata, H., Amano, M., Das, D., et al. (2011). Loss of protease dimerization inhibition activity of darunavir is associated with the acquisition of resistance to darunavir by HIV-1. *J. Virol.* 85, 10079–10089. doi: 10.1128/JVI.05121-11

Koh, Y., Matsumi, S., Das, D., Amano, M., Davis, D. A., Li, J., et al. (2007). Potent inhibition of HIV-1 replication by novel non-peptidyl small molecule inhibitors of protease dimerization. *J. Biol. Chem.* 282, 28709–28720. doi: 10.1074/jbc.M703938200

Koh, Y., Nakata, H., Maeda, K., Ogata, H., Bilcer, G., Devasamudram, T., et al. (2003). Novel bis-tetrahydrofuranylurethane-containing nonpeptidic protease inhibitor (PI) UIC-94017 (TMC114) with potent activity against multi-PI-resistant human immunodeficiency virus *in vitro*. *Antimicrob. Agents Chemother.* 47, 3123–3129. doi: 10.1128/AAC.47.10.3123-3129.2003

Kovalevsky, A. Y., Tie, Y., Liu, F., Boross, P. I., Wang, Y. F., Leshchenko, S., et al. (2006). Effectiveness of nonpeptide clinical inhibitor TMC-114 on HIV-1 protease with highly drug resistant mutations D30N, I50V, and L90M. *J. Med. Chem.* 49, 1379–1387. doi: 10.1021/jm050943c

Krohn, A., Redshaw, S., Ritchie, J. C., Graves, B. J., and Hatada, M. H. (1991). Novel binding mode of highly potent HIV-proteinase inhibitors incorporating the (R)-hydroxyethylamine isostere. *J. Med. Chem.* 34, 3340–3342.

Lam, P. Y., Jadhav, P. K., Eyermann, C. J., Hodge, C. N., Ru, Y., Bacheler, L. T., et al. (1994). Rational design of potent, bioavailable, nonpeptide cyclic ureas as HIV protease inhibitors. *Science* 263, 380–384.

Liu, F., Boross, P. I., Wang, Y. F., Tozser, J., Louis, J. M., Harrison, R. W., et al. (2005). Kinetic, stability, and structural changes in high-resolution crystal structures of HIV-1 protease with drug-resistant mutations L24I, I50V, and G73S. *J. Mol. Biol.* 354, 789–800. doi: 10.1016/j.jmb.2005.09.095

Liu, F., Kovalevsky, A. Y., Tie, Y., Ghosh, A. K., Harrison, R. W., and Weber, I. T. (2008). Effect of flap mutations on structure of HIV-1 protease and inhibition by saquinavir and darunavir. *J. Mol. Biol.* 381, 102–115. doi: 10.1016/j.jmb.2008.05.062

Maguire, M. F., Guinea, R., Griffin, P., MacManus, S., Elston, R. C., Wolfram, J., et al. (2002). Changes in human immunodeficiency virus type 1 Gag at positions L449 and P453 are linked to I50V protease mutants *in vivo* and cause reduction of sensitivity to amprenavir and improved viral fitness *in vitro*. *J. Virol.* 76, 7398–7406. doi: 10.1128/JVI.76.15.7398-7406.2002

Martin, P., Vickrey, J. F., Proteasa, G., Jimenez, Y. L., Wawrzak, Z., Winters, M. A., et al. (2005). "Wide-open" 1.3 A structure of a multidrug-resistant HIV-1 protease as a drug target. *Structure* 13, 1887–1895. doi: 10.1016/j.str.2005.11.005

Mittal, S., Bandaranayake, R. M., King, N. M., Prabu-Jeyabalan, M., Nalam, M. N., Nalivaika, E. A., et al. (2013). Structural and thermodynamic basis of amprenavir/darunavir and atazanavir resistance in HIV-1 protease with mutations at residue 50. *J. Virol.* 87, 4176–4184. doi: 10.1128/JVI.03486-12

Murshudov, G. N., Vagin, A. A., and Dodson, E. J. (1997). Refinement of macromolecular structures by the maximum-likelihood method. *Acta Crystallogr. D Biol. Crystallogr.* 53, 240–255. doi: 10.1107/S0907444996012255

Ode, H., Matsuyama, S., Hata, M., Hoshino, T., Kakizawa, J., and Sugiura, W. (2007a). Mechanism of drug resistance due to N88S in CRF01_AE HIV-1 protease, analyzed by molecular dynamics simulations. *J. Med. Chem.* 50, 1768–1777. doi: 10.1021/jm061158i

Ode, H., Matsuyama, S., Hata, M., Neya, S., Kakizawa, J., Sugiura, W., et al. (2007b). Computational characterization of structural role of the non-active site mutation M36I of human immunodeficiency virus type 1 protease. *J. Mol. Biol.* 370, 598–607. doi: 10.1016/j.jmb.2007.04.081

Otwinowski, Z., and Minor, W. (1997). Processing of X-Ray diffraction data collected in oscillation mode. *Meth. Enzymol.* 276, 307–326.

Pazhanisamy, S., Stuver, C. M., Cullinan, A. B., Margolin, N., Rao, B. G., and Livingston, D. J. (1996). Kinetic characterization of human immunodeficiency virus type-1 protease-resistant variants. *J. Biol. Chem.* 271, 17979–17985.

Perryman, A. L., Lin, J. H., and McCammon, J. A. (2004). HIV-1 protease molecular dynamics of a wild-type and of the V82F/I84V mutant: possible contributions to drug resistance and a potential new target site for drugs. *Protein Sci.* 13, 1108–1123. doi: 10.1110/ps.03468904

Prabu-Jeyabalan, M., Nalivaika, E., and Schiffer, C. A. (2002). Substrate shape determines specificity of recognition for HIV-1 protease: analysis of crystal structures of six substrate complexes. *Structure* 10, 369–381. doi: 10.1016/S0969-2126(02)00720-7

Prado, J. G., Wrin, T., Beauchaine, J., Ruiz, L., Petropoulos, C. J., Frost, S. D., et al. (2002). Amprenavir-resistant HIV-1 exhibits lopinavir cross-resistance and reduced replication capacity. *AIDS* 16, 1009–1017. doi: 10.1097/00002030-200205030-00007

Rhee, S. Y., Taylor, J., Fessel, W. J., Kaufman, D., Towner, W., Troia, P., et al. (2010). HIV-1 protease mutations and protease inhibitor cross-resistance. *Antimicrob. Agents Chemother.* 54, 4253–4261. doi: 10.1128/AAC.00574-10

Saskova, K. G., Kozisek, M., Rezacova, P., Brynda, J., Yashina, T., Kagan, R. M., et al. (2009). Molecular characterization of clinical isolates of human immunodeficiency virus resistant to the protease inhibitor darunavir. *J. Virol.* 83, 8810–8818. doi: 10.1128/JVI.00451-09

Schapiro, J. M., Scherer, J., Boucher, C. A., Baxter, J. D., Tilke, C., Perno, C. F., et al. (2010). Improving the prediction of virological response to tipranavir: the development and validation of a tipranavir-weighted mutation score. *Antivir. Ther.* 15, 1011–1019. doi: 10.3851/IMP1670

Shibata, J., Sugiura, W., Ode, H., Iwatani, Y., Sato, H., Tsang, H., et al. (2011). Within-host co-evolution of Gag P453L and protease D30N/N88D demonstrates virological advantage in a highly protease inhibitor-exposed HIV-1 case. *Antiviral Res.* 90, 33–41. doi: 10.1016/j.antiviral.2011.02.004

Spinelli, S., Liu, Q. Z., Alzari, P. M., Hirel, P. H., and Poljak, R. J. (1991). The three-dimensional structure of the aspartyl protease from the HIV-1 isolate BRU. *Biochimie* 73, 1391–1396.

Surleraux, D. L., Tahri, A., Verschueren, W. G., Pille, G. M., de Kock, H. A., Jonckers, T. H., et al. (2005). Discovery and selection of TMC114, a next generation HIV-1 protease inhibitor. *J. Med. Chem.* 48, 1813–1822. doi: 10.1021/jm049560p

Thaisrivongs, S., Skulnick, H. I., Turner, S. R., Strohbach, J. W., Tommasi, R. A., Johnson, P. D., et al. (1996). Structure-based design of HIV protease inhibitors: sulfonamide-containing 5,6-dihydro-4-hydroxy-2-pyrones as non-peptidic inhibitors. *J. Med. Chem.* 39, 4349–4353. doi: 10.1021/jm960541s

Tremblay, C. L. (2008). Combating HIV resistance–focus on darunavir. *Ther. Clin. Risk Manag.* 4, 759–766.

Vargin, A., and Teplyakov, A. (1997). MOLREP: an automated program for molecular replacement. *J. Appl. Crystallogr.* 30, 1022–1025.

Wang, J., Wolf, R. M., Caldwell, J. W., Kollman, P. A., and Case, D. A. (2004). Development and testing of a general amber force field. *J. Comput. Chem.* 25, 1157–1174. doi: 10.1002/jcc.20035

Wensing, A. M., Calvez, V., Gunthard, H. F., Johnson, V. A., Paredes, R., Pillay, D., et al. (2014). 2014 Update of the drug resistance mutations in HIV-1. *Top. Antivir. Med.* 22, 642–650.

Winn, M. D., Ballard, C. C., Cowtan, K. D., Dodson, E. J., Emsley, P., Evans, P. R., et al. (2011). Overview of the CCP4 suite and current developments. *Acta Crystallogr. D Biol. Crystallogr.* 67, 235–242. doi: 10.1107/S0907444910045749

Zhang, Y., Chang, Y. C., Louis, J. M., Wang, Y. F., Harrison, R. W., and Weber, I. T. (2014). Structures of darunavir-resistant HIV-1 protease mutant reveal atypical binding of darunavir to wide open flaps. *ACS Chem. Biol.* 9, 1351–1358. doi: 10.1021/cb4008875

**Conflict of Interest Statement:** The authors declare that the research was conducted in the absence of any commercial or financial relationships that could be construed as a potential conflict of interest.

The reviewer YTY declared a shared affiliation, though no other collaboration, with one of the authors MF to the handling Editor, who ensured that the process nevertheless met the standards of a fair and objective review.

INTERNAL MEDICINE

CASE REPORT

# An Hepatitis C Virus (HCV)/HIV Co-Infected Patient who Developed Severe Hepatitis during Chronic HCV Infection: Sustained Viral Response with Simeprevir Plus Peginterferon-Alpha and Ribavirin

Noboru Hirashima[1], Hiroaki Iwase[1], Masaaki Shimada[1], Junji Imamura[2], Wataru Sugiura[2], Yoshiyuki Yokomaku[2] and Tsunamasa Watanabe[2,3]

## Abstract

We herein describe the case of a 42-year-old man who developed severe hepatitis caused by hepatitis C virus (HCV) infection at 14 years after the start of human immunodeficiency virus (HIV) treatment. Surprisingly, the levels of alanine aminotransferase (ALT) fluctuated, reaching a peak higher than 1,000 IU/L during chronic HCV infection, and the hepatic histology showed advanced liver fibrosis at 3 years after the primary HCV infection. He was treated with simeprevir, peginterferon-alpha, and ribavirin with a sustained viral response. We conclude that HCV/HIV co-infected patients need to commence anti-HCV therapy when the levels of ALT fluctuate severely under successful HIV control.

**Key words:** hepatitis C virus, human immunodeficiency virus, co-infection, simeprevir, peginterferon-alpha, severe hepatitis

**(Intern Med 54: 2173-2177, 2015)**
**(DOI: 10.2169/internalmedicine.54.4344)**

## Introduction

Co-infection with hepatitis C virus (HCV) and human immunodeficiency virus (HIV) is common, as both viruses share similar modes of transmission (1). Although injection drug use (IDU) remains the main route of HCV infection, recent studies have shown that HCV can be sexually transmitted in the absence of IDU, particularly among HIV-positive men who have sex with men (MSM) (2-5). In general, the progression of HCV-related liver diseases is accelerated in HCV/HIV co-infected individuals (6, 7). HCV has emerged as an important cause of morbidity and mortality in co-infected patients (8) because successful combination antiretroviral therapy (cART) has dramatically changed the prognosis of HIV-infected individuals (9). The consequences of HCV/HIV co-infection are less spontaneous clearance (10), higher rates of chronicity, accelerated fibrosis progression with increased risk of cirrhosis (11, 12) and hepatocellular carcinoma (13) resulting in higher liver-related mortality, and decreased HCV treatment response (14, 15). The management of HCV infection among the HIV-infected population poses a serious challenge for physicians. Recently, a better sustained viral response (SVR) has been seen following combination therapy of HCV protease inhibitor simeprevir and peginterferon-alpha/ribavirin (PegIFNα/RBV) (16). This combination therapy may be a suitable treatment regimen for HCV-positive Japanese patients because the interferon-resistant HCV genotype 1b is more common in Japan (17). This report herein describes a case of a MSM who developed severe hepatitis caused by chronic HCV infection while under successful cART, and who achieved SVR through HCV treatment with simeprevir and PegIFNα/RBV.

[1]Department of Gastroenterology, National Hospital Organization Nagoya Medical Center, Japan, [2]Department of Infectious Diseases and Immunology Clinical Research Center, National Hospital Organization Nagoya Medical Center, Japan and [3]Department of Virology and Liver Unit, Nagoya City University Graduate School of Medical Sciences, Japan
Received for publication October 22, 2014; Accepted for publication December 25, 2014
Correspondence to Dr. Tsunamasa Watanabe, twatanab@marianna-u.ac.jp

**Table. Laboratory Data before Treatment of Hepatitis C.**

| Blood cells | | Blood chemistry | | Serological test | |
|---|---|---|---|---|---|
| RBCs | $557\times10^4$ /μL | Albumin | 4.4 g/dL | HBs antigen | 0.01 mIU/mL (negative) |
| Hemoglobin | 16.2 g/dL | AST | 32 IU/L | HBs antibody | 219.93 mIU/mL (positive) |
| Hematocrit | 48.3% | ALT | 49 IU/L | HBc antibody | 4.40 Sample/c (positive) |
| WBCs | 5,200 /μL | Alkaline phosphatase | 187 IU/L | HBV DNA | not detected |
| Neutrophils | 55.9% | γ-glutamyl transferase | 112 IU/L | HCV antibody | 10.69 Sample/c (positive) |
| Lymphocytes | 29.6% | Total bilirubin | 1.4 mg/dL | HCV serotype | undetermined |
| Platelets | $15.5\times10^4$ /μL | Blood urea nitrogen | 10 mg/dL | HCV RNA | 6.8 Log IU/mL |
| CD4 cells | 376 /μL | Creatinine | 0.79 mg/dL | HIV-1 RNA | not detected |
| CD4/CD8 ratio | 1.0 | Hyaluronic acid | 148 ng/mL (<50) | *IL 28B* SNP | Major homo |
| PT (INR) | 1.24 | PIIINP | 1.2 U/mL (<1.0) | α fetoprotein | 6 ng/mL |
| | | Type IV collagen 7S | 8.4 ng/mL (<6.0) | PIVKA II | 24 mAU/mL |

RBC: red blood cell, WBC: white blood cell, AST: aspartate aminotransferase, ALT: alanine aminotransferase, PIIINP: amino-terminal properties of type III collagen, PT (INR): prothrombin time (International Normalized Rate)

## Case Report

A 42-year-old Japanese man was diagnosed with an HIV-1 infection at our hospital in August 1997. He is a MSM and had no other risk of liver damage (e.g., ingestion of alcohol or the presence of diabetes mellitus). At his initial laboratory examination, his HIV-1 viral load was 75,000 copies (3.8 log copies)/mL, and his CD4-positive cell count was 160/μL. The patient began treatment with two nucleoside analogue reverse transcriptase inhibitors (NRTIs) in 1997, which was common before treatment with cART was established and is now contraindicated. Nelfinavir was added to his treatment regimen after its approval by the Japanese Ministry of Health and Welfare in 1998; however, this treatment failed because of viral drug resistance. The nelfinavir-related resistant amino acid mutation D30N was detected on his HIV drug resistance test. The subsequent regimen consisted of didanosine (ddI), abacavir (ABC), and ritonavir-boosted atazanavir; these drugs were selected for salvage treatment and afterwards, the virus was well controlled. In 2011, the cART regimen was updated to ABC, etravirine (ETR), and raltegravir (RAL) to aid in preventing ddI long-term toxicity, lactic acidosis due to mitochondria injury, lipodystrophy, neuropathy, and portal vein embolization. The patient's HIV viral load was undetectable and his CD4 count was maintained above 350/μL for 15 years after the salvage treatment was initiated. At 14 years after the introduction of antiretroviral treatment, his alanine aminotransferase (ALT) and aspartate aminotransferase (AST) levels rose to 601 IU/L and 268 IU/L, respectively, and the anti-HCV antibody was seroconverted, thus leading to the clinical diagnosis of acute HCV infection. There was no evidence of hepatitis A, B, D, or E infection, or evidence of other causes of haptic cytolysis; the patient reported having had unprotected receptive anal intercourse with multiple men the previous year but had never injected illicit drugs. His HCV RNA load was 6.3 log IU/mL, however, the HCV serotype was indeterminable. One month after the onset of acute hepatitis, his ALT level decreased to under 200 IU/L and further decreased to less than 100 IU/L after 4 months. Because his platelet count was over 180,000/μL and the noninvasive biomarkers of liver fibrosis (18, 19) did not indicate advanced liver fibrosis [hyaluronic acid: 60.7 μg/L (normal: <50 μg/L), amino-terminal properties of type III collagen: 1.1 U/mL (normal: <1.0 U/mL), type IV collagen 7S: 5.3 ng/mL (normal: <6.0 ng/mL)], the HCV treatment was suspended until direct-acting antivirals (DAAs), which are highly effective, well-tolerated therapies (20), were approved by the Japanese Ministry of Health, Labour and Welfare. Two years after the onset of his primary HCV infection, the patient's liver transaminases were again elevated (ALT 1,100 IU/L, AST 541 IU/L) and the exacerbation of his HCV infection was supported by HCV RNA fluctuations (his HCV load was 6.2 to 7.2 log IU/mL). A percutaneous liver biopsy was performed 3 years after the diagnosis of his primary HCV infection and indicated advanced fibrosis with active hepatitis (grade 3 inflammation and stage 3 fibrosis based on the New Inuyama Classification), but no steatohepatitis or other type of liver injury was observed. The patient was treated with simeprevir and PegIFNα-2b/RBV for 24 weeks while estimating the presence of HCV genotype 1 infection, because the result of HCV serotyping by an enzyme-linked immunosorbent assay using group-specific recombinant peptides for the NS4 region (21) was undetermined. The cART regimen was changed to rilpivirine (RPV)/RAL for HCV treatment, because both RPV and RAL have relatively few drug-drug interactions with simeprevir. The patient achieved SVR without severe complications (including possible HIV virological rebound) and his ALT level returned to within the normal range. The laboratory data before the start of HCV therapy is summarized in Table. *IL28B* single nucleotide polymorphisms (TT genotype) were found (22). The overview of the clinical course of our case is shown in Figure.

## Discussion

Elevated ALT levels against primary HCV infection are reported to be mild and relatively transient in HIV-infected MSM (23). The present case is a MSM who showed HCV seroconversion with a high ALT level (elevated to 601 IU/L)

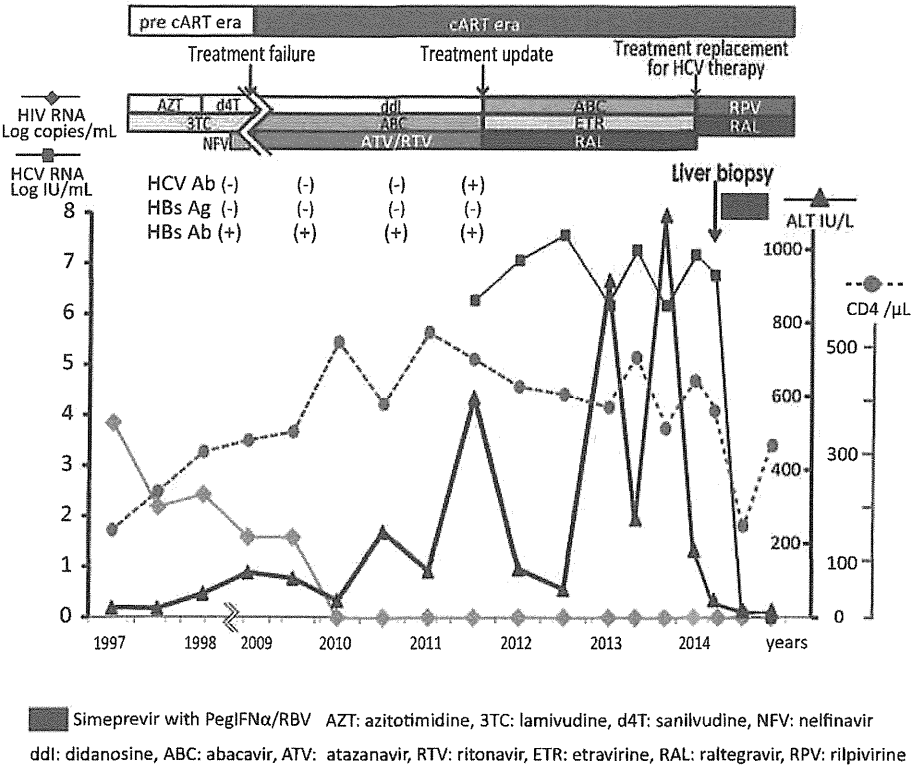


**Figure. The clinical course of our case.**

under successful cART. Surprisingly, his ALT levels fluctuated and elevated to over 1,000 IU/L 2 years after his primary HCV infection. In general, chronic hepatitis caused by HCV mono-infection exhibits a mild increase in ALT, rarely over 300 IU/L, because HCV-specific T-cell responses became dysfunctional over several months after the primary infection (24, 25). Moreover, during HIV infection, impaired CD4+ T-cells function and the subsequent depletion of CD4+ T-cells, as a result of continuous CD4+ cell destruction, is thought to be a cause of the profound impaired cellular immune response which has an important role in viral hepatitis. However, in this HCV/HIV co-infected patient, his liver inflammation two years after the primary HCV infection represented severe hepatitis (ALT levels peaking at > 1,000 IU/L) beyond the chronic HCV mono-infected conditions. These findings indicated that the immune responses against HCV infection could not completely recover in HIV-infected individuals even after long-term treatment with successful cART regimens. HIV infection is well known as an immune suppressive disease but its essentially an immune disorder. Many clinicians actually face diverse immune disorders, including not only immune suppressive disease characterized by a susceptibility to infection with opportunistic pathogens, but also autoimmune diseases (such as thyroid diseases, psoriasis, systemic lupus erythematodes, and inflammatory bowel syndrome) after the immune system recovers following cART. The causes of induced autoimmune diseases remain unknown, however, it is believed that functional impairments on regulatory T-cells (Tregs), sustained even after starting cART, contributes to induce dysregulated inflammation. Therefore, we hypothesize that the reason for a strong cellular immune response during HIV infection is due to the fact that CD4+ Tregs can be infected with HIV-1 (26), and the Treg function may not have fully recovered even though the patient's HIV infection had been well controlled by successful cART regimens for more than 15 years. Although direct evidence for this hypothesis is lacking, it was previously reported that impaired Treg function may have detrimental consequences for the control of HCV immune activation (27) and accelerated fibrosis progression. Indeed, our patient's hepatic histology 3 years after the primary HCV infection presented as F3 (pre-cirrhosis stage), indicating the very rapid progression of liver fibrosis from the HCV infection in an HIV-infected individual even though the CD4+ T-cell counts recovered. Therefore, careful monitoring for the rapid progression of hepatitis C is required for HIV-infected individuals even after successful HIV control.

In HCV/HIV co-infected patients, cART has shown to delay the progression of liver cirrhosis (28), and those with undetectable HIV RNA levels tend to have slower cirrhosis progression than those with detectable viremia (29). However, in the present case, the HIV RNA levels were repeatedly undetectable, and the hepatic histology showed the development of pre-cirrhosis due to severe liver inflammation. Therefore, treating the HCV with active hepatitis was required to halt the fibrosis progression. The response to treatment with PegIFNα/RBV in HCV/HIV co-infected patients is poorer than that of patients with HCV mono-infection. In fact, the SVR rate is reported to be 27-29% (30-32) in co-

infected patients compared with 42-46% (33, 34) in HCV genotype 1 mono-infections. It is expected that DAA will be a good therapy for HCV/HIV co-infected individuals. Co-infected patients receiving concurrent HIV and HCV treatment, however, are faced with the difficulty of proper treatment regimen selection, such as an increased risk of drug-drug interactions and drug-induced liver injury, particularly among those with advanced liver disease (35). HIV integrase inhibitors (i.e., RAL) have relatively few drug-drug interactions, whereas the use of HIV protease inhibitors and non-nucleoside reverse transcriptase inhibitor (NNRTI), except RPV, might preclude the use of some HCV DAA agents, particularly those targeting HCV protease. The patients are sometimes forced to change cART regimens because HCV proteases are metabolized through CYP3A4 and HIV protease inhibitors and NNRTIs interfere with the CYP3A4 activity, which may affect the HCV protease blood concentration. Therefore, we selected RAL and RPV as the NRTI-sparing regimen, because RPV has fewer drug-drug interactions and this combination is effective for HIV suppression with minimal side effects. In a phase II study, treatment with telaprevir (a first-generation HCV NS3/4A protease inhibitor) and PegIFNα/RBV for 48 weeks led to significantly greater responses in HCV/HIV co-infected patients, with SVR rates of 74% (36). The second-generation HCV protease inhibitor simeprevir, a once-daily HCV protease inhibitor with more favorable tolerability, has also been studied in co-infected populations. When given for 12 weeks in combination with PegIFNα/RBV to co-infected individuals with HCV genotype 1, the overall SVR at 12 weeks was 74% (37). Because simeprevir can interact with HIV protease inhibitors and efavirenz (an NNRTI), most patients in that study were placed on RAL-based cART.

For many patients, it is clear that there is a benefit to waiting for the approval of new DAA agents as interferon-free treatment regimens. However, immediate HCV therapy should be strongly considered for co-infected patients with advanced fibrosis or active hepatitis. For HCV treatment-naive co-infected patients, we recommend that immediate cART initiation should be considered and the degree of fibrosis should be examined in each patient. A liver biopsy may be required for the co-infected patients, because reduced platelet counts are more commonly observed among patients infected with HIV (38, 39) and noninvasive scoring systems are still in the early use in HIV co-infected patients.

In conclusion, HCV/HIV co-infected patients under successful HIV control, especially those with primary HCV infection after HIV infection, must be carefully monitored to evaluate both the progression of hepatitis and the initiation of anti-HCV therapy, even if the noninvasive biomarkers of liver fibrosis indicate decreased fibrosis.

**The authors state that they have no Conflict of Interest (COI).**

## References


1. Alter MJ. Epidemiology of viral hepatitis and HIV co-infection. J Hepatol **44**: S6-S9, 2006.
2. Urbanus AT, van de Laar TJ, Stolte IG, et al. Hepatitis C virus infections among HIV-infected men who have sex with men: an expanding epidemic. AIDS **23**: F1-F7, 2009.
3. van de Laar T, Pybus O, Bruisten S, et al. Evidence of a large, international network of HCV transmission in HIV-positive men who have sex with men. Gastroenterology **136**: 1609-1617, 2009.
4. Matthews GV, Pham ST, Hellard M, et al. Patterns and characteristics of hepatitis C transmission clusters among HIV-positive and HIV-negative individuals in the Australian trial in acute hepatitis C. Clin Infect Dis **52**: 803-811, 2011.
5. Fierer DS, Dieterich DT, Fiel MI, et al. Rapid progression to decompensated cirrhosis, liver transplant, and death in HIV-infected men after primary hepatitis C virus infection. Clin Infect Dis **56**: 1038-1043, 2013.
6. Thein HH, Yi Q, Dore GJ, Krahn MD. Natural history of hepatitis C virus infection in HIV-infected individuals and the impact of HIV in the era of highly active antiretroviral therapy: a meta-analysis. AIDS **22**: 1979-1991, 2008.
7. Martin-Carbonero L, Benhamou Y, Puoti M, et al. Incidence and predictors of severe liver fibrosis in human immunodeficiency virus-infected patients with chronic hepatitis C: a European collaborative study. Clin Infect Dis **38**: 128-133, 2004.
8. Chen TY, Ding EL, Seage Iii GR, Kim AY. Meta-analysis: increased mortality associated with hepatitis C in HIV-infected persons is unrelated to HIV disease progression. Clin Infect Dis **49**: 1605-1615, 2009.
9. Kitahata MM, Gange SJ, Abraham AG, et al. Effect of early versus deferred antiretroviral therapy for HIV on survival. N Engl J Med **360**: 1815-1826, 2009.
10. Sulkowski MS. Hepatitis C virus infection in HIV-infected patients. Curr Infect Dis Rep **3**: 469-476, 2001.
11. Pineda JA, Romero-Gomez M, Diaz-Garcia F, et al. HIV coinfection shortens the survival of patients with hepatitis C virus-related decompensated cirrhosis. Hepatology **41**: 779-789, 2005.
12. Pineda JA, Aguilar-Guisado M, Rivero A, et al. Natural history of compensated hepatitis C virus-related cirrhosis in HIV-infected patients. Clin Infect Dis **49**: 1274-1282, 2009.
13. Brau N, Fox RK, Xiao P, et al. Presentation and outcome of hepatocellular carcinoma in HIV-infected patients: a U.S.-Canadian multicenter study. J Hepatol **47**: 527-537, 2007.
14. Torriani FJ, Rodriguez-Torres M, Rockstroh JK, et al. Peginterferon Alfa-2a plus ribavirin for chronic hepatitis C virus infection in HIV-infected patients. N Engl J Med **351**: 438-450, 2004.
15. Rodriguez-Torres M, Slim J, Bhatti L, et al. Peginterferon alfa-2a plus ribavirin for HIV-HCV genotype 1 coinfected patients: a randomized international trial. HIV Clin Trials **13**: 142-152, 2012.
16. Jacobson IM, Dore GJ, Foster GR, et al. Simeprevir with pegylated interferon alfa 2a plus ribavirin in treatment-naive patients with chronic hepatitis C virus genotype 1 infection (QUEST-1): a phase 3, randomised, double-blind, placebo-controlled trial. Lancet **384**: 403-413, 2014.
17. Izumi N, Hayashi N, Kumada H, et al. Once-daily simeprevir with peginterferon and ribavirin for treatment-experienced HCV genotype 1-infected patients in Japan: the CONCERTO-2 and CONCERTO-3 studies. J Gastroenterol **49**: 941-953, 2014.
18. Stauber RE, Lackner C. Noninvasive diagnosis of hepatic fibrosis in chronic hepatitis C. World J Gastroenterol **13**: 4287-4294, 2007.
19. Cacoub P, Carrat F, Bedossa P, et al. Comparison of non-invasive liver fibrosis biomarkers in HIV/HCV co-infected patients: the fibrovic study--ANRS HC02. J Hepatol **48**: 765-773, 2008.
20. Chatel-Chaix L, Germain MA, Gotte M, Lamarre D. Direct-acting

and host-targeting HCV inhibitors: current and future directions. Curr Opin Virol **2**: 588-598, 2012.

**21.** Tanaka T, Tsukiyama-Kohara K, Yamaguchi K, et al. Significance of specific antibody assay for genotyping of hepatitis C virus. Hepatology **19**: 1347-1353, 1994.

**22.** Tanaka Y, Nishida N, Sugiyama M, et al. Genome-wide association of IL28B with response to pegylated interferon-alpha and ribavirin therapy for chronic hepatitis C. Nat Genet **41**: 1105-1109, 2009.

**23.** van de Laar TJ, Matthews GV, Prins M, Danta M. Acute hepatitis C in HIV-infected men who have sex with men: an emerging sexually transmitted infection. AIDS **24**: 1799-1812, 2010.

**24.** Dustin LB, Rice CM. Flying under the radar: the immunobiology of hepatitis C. Annu Rev Immunol **25**: 71-99, 2007.

**25.** Rehermann B, Nascimbeni M. Immunology of hepatitis B virus and hepatitis C virus infection. Nat Rev Immunol **5**: 215-229, 2005.

**26.** Pion M, Jaramillo-Ruiz D, Martinez A, Munoz-Fernandez MA, Correa-Rocha R. HIV infection of human regulatory T cells downregulates Foxp3 expression by increasing DNMT3b levels and DNA methylation in the FOXP3 gene. AIDS **27**: 2019-2029, 2013.

**27.** Williams SK, Donaldson E, Van der Kleij T, et al. Quantification of hepatic FOXP3+ T-lymphocytes in HIV/hepatitis C coinfection. J Viral Hepat **21**: 251-259, 2014.

**28.** Qurishi N, Kreuzberg C, Luchters G, et al. Effect of antiretroviral therapy on liver-related mortality in patients with HIV and hepatitis C virus coinfection. Lancet **362**: 1708-1713, 2003.

**29.** Macias J, Berenguer J, Japon MA, et al. Fast fibrosis progression between repeated liver biopsies in patients coinfected with human immunodeficiency virus/hepatitis C virus. Hepatology **50**: 1056-1063, 2009.

**30.** Sulkowski M, Pol S, Mallolas J, et al. Boceprevir versus placebo with pegylated interferon alfa-2b and ribavirin for treatment of hepatitis C virus genotype 1 in patients with HIV: a randomised, double-blind, controlled phase 2 trial. Lancet Infect Dis **13**: 597-605, 2013.

**31.** Carrat F, Bani-Sadr F, Pol S, et al. Pegylated interferon alfa-2b vs standard interferon alfa-2b, plus ribavirin, for chronic hepatitis C in HIV-infected patients: a randomized controlled trial. JAMA **292**: 2839-2848, 2004.

**32.** Chung RT, Andersen J, Volberding P, et al. Peginterferon Alfa-2a plus ribavirin versus interferon alfa-2a plus ribavirin for chronic hepatitis C in HIV-coinfected persons. N Engl J Med **351**: 451-459, 2004.

**33.** Manns MP, McHutchison JG, Gordon SC, et al. Peginterferon alfa-2b plus ribavirin compared with interferon alfa-2b plus ribavirin for initial treatment of chronic hepatitis C: a randomised trial. Lancet **358**: 958-965, 2001.

**34.** Fried MW, Shiffman ML, Reddy KR, et al. Peginterferon alfa-2a plus ribavirin for chronic hepatitis C virus infection. N Engl J Med **347**: 975-982, 2002.

**35.** Aranzabal L, Casado JL, Moya J, et al. Influence of liver fibrosis on highly active antiretroviral therapy-associated hepatotoxicity in patients with HIV and hepatitis C virus coinfection. Clin Infect Dis **40**: 588-593, 2005.

**36.** Sulkowski MS, Sherman KE, Dieterich DT, et al. Combination therapy with telaprevir for chronic hepatitis C virus genotype 1 infection in patients with HIV: a randomized trial. Ann Intern Med **159**: 86-96, 2013.

**37.** Dieterich D, Rockstroh JK, Orkin C, et al. Simeprevir (TMC435) with peginterferon/ribavirin in patients coinfected with HCV genotype-1 and HIV-1: a phase 3 study. Clin Infect Dis **59**: 1579-1587, 2014.

**38.** Bambha K, Pierce C, Cox C, et al. Assessing mortality in women with hepatitis C virus and HIV using indirect markers of fibrosis. AIDS **26**: 599-607, 2012.

**39.** Nunes D, Fleming C, Offner G, et al. HIV infection does not affect the performance of noninvasive markers of fibrosis for the diagnosis of hepatitis C virus-related liver disease. J Acquir Immune Defic Syndr **40**: 538-544, 2005.

INTERNAL MEDICINE

CASE REPORT

# Corticoid Therapy for Overlapping Syndromes in an HIV-positive Patient

Yu Kaku, Shoko Kodama, Makiko Higuchi, Akihiro Nakamura, Masataka Nakamura, Tomoe Kaieda, Soichiro Takahama, Rumi Minami, Tomoya Miyamura, Eiichi Suematsu and Masahiro Yamamoto

## Abstract

Human immunodeficiency virus (HIV) infection disturbs the host's immune function and often coexists with various autoimmune and/or systemic rheumatic diseases with manifestations that sometimes overlap with each other. We herein present the case of a 43-year-old Japanese man infected with HIV who exhibited elevated serum creatine kinase and transaminases levels without any symptoms. He was diagnosed with autoimmune hepatitis, polymyositis and Sjögren's syndrome and received combined antiretroviral therapy (cART); however, the laboratory abnormalities persisted. We successfully administered cART with the addition of oral prednisolone, and the patient's condition recovered without side effects related to the metabolic or immunosuppressive effects of these drugs.

**Key words:** human immunodeficiency virus (HIV), polymyositis (PM), Sjögren's syndrome (SS), autoimmune hepatitis (AIH), steroid, combined antiretroviral therapy (cART)

**(Intern Med 54: 223-230, 2015)**
**(DOI: 10.2169/internalmedicine.54.3094)**

## Introduction

Human immunodeficiency virus (HIV)-infected patients sometimes present with a variety of autoimmune manifestations generated by the polyclonal stimulation of B cells and development of hypergammaglobulinemia (1). It has been reported that 4-71% of HIV-positive patients complain of rheumatic symptoms (2). HIV-infected individuals may develop multiple forms of autoimmune dysfunction, including vasculitis, rheumatologic conditions, HIV-associated connective tissue diseases and musculoskeletal disorders, such as arthritis/arthralgia or myalgia. Comorbid diseases include rheumatoid arthritis (RA), dermatomyositis (DM)/polymyositis (PM), systemic lupus erythematosus (SLE) and Sjögren's syndrome (SS).

In addition, systemic rheumatic diseases are known to coincide with each other and/or other autoimmune disorders, including autoimmune adrenal insufficiency (Addison's disease), autoimmune hepatitis (AIH), autoimmune thyroid disease, antiphospholipid syndrome, biliary inflammatory diseases such as primary sclerosing cholangitis and primary biliary cirrhosis, celiac disease, inflammatory bowel diseases such as ulcerative colitis and Crohn's disease, myasthenia gravis, sarcoidosis, type 1 diabetes mellitus and vasculitis (3).

Furthermore, HIV infection is often associated with various laboratory abnormalities, including the presence of antinuclear antibodies (ANA), antiplatelet antibodies, antilymphocyte antibodies, antigranulocyte antibodies or antiphospholipid antibodies and positive tests for direct antiglobulin (Coombs test), circulating immune complexes, rheumatoid factor or cryoglobulin. These autoimmune manifestations are generated by the polyclonal stimulation of B cells and development of hypergammaglobulinemia (1), as well as a state of predominant CD8 T cells and/or immune reconstitution due to effective treatment with combined antiretroviral therapy (cART) (4). However, it is very rare for HIV infection to coexist with two or more rheumatic and/or autoimmune conditions.

Department of Internal Medicine, Clinical Research Institute, National Hospital Organization Kyushu Medical Center, Japan
Received for publication April 15, 2014; Accepted for publication June 8, 2014
Correspondence to Dr. Masahiro Yamamoto, inb@kyumed.jp